

Appendix E. Supporting Analyses for Section 2.0

E.1 LDW HYDROLOGY

A Log-Pearson Type 3 high-flow event frequency analysis (Helsel and Hirsch 2002) of daily-average flow rate data collected at the Green River gauging station was conducted. The Log-Pearson Type 3 analysis is the recommended technique for high-flow event frequency analysis (IACDWD 1982). The analysis was conducted as follows:

- ◆ Determine the annual peak discharge (i.e., daily-average flow rate) for the period of record. For this analysis, Green River discharge data collected from 1961 through 2004 were used, which constituted a 44-year period of record.
- ◆ The logarithm of each annual peak discharge during the 44-year period was calculated.
- ◆ For the logarithms of annual peak discharge, these statistics were calculated: mean (M), standard deviation (S), and skewness (g).
- ◆ The peak discharge (Q_p) for a specific annual exceedance probability (AEP) was calculated using:

$$\text{Log}(Q_p) = M + KS \quad (\text{Equation E-1})$$

where $\log(Q_p)$ is the logarithm of the peak discharge with an AEP of 1 in Y years and K is the frequency factor for a specific AEP as a function of skewness (g). Tabulated values of K are presented in Helsel and Hirsch (2002). For example, AEP values of 10% and 1% correspond to high-flow events with return periods of 10 and 100 years, respectively.

The results of this analysis indicate that high-flow event discharges range from 8,400 cfs for a 2-yr high-flow event to 12,000 cfs for a 100-yr high-flow event (see Figure 2-1). The relatively low range in river discharge is because of flow control at the Howard Hansen Dam upstream of the LDW. The frequency of occurrence of various high-flow events is presented in Figure E-1. In that figure, frequency of occurrence corresponds to the number of days during the period of record that daily-average flow rate is within a specific high-flow discharge range. Time histories of daily-average flow rate in the Green River from 1961 through 2004 are shown in Figures E-2 through E-12. Also shown on these figures are discharge values for various high-flow events (e.g., 2-yr high-flow event), making it possible to determine the frequency of occurrence of high-flow events with different return periods since 1961.

E.2 GRAIN SIZE DISTRIBUTION DATA

Previous field studies have acquired grain size distribution data in the surface layer sediments. These data provide information on the clay, silt and sand content in the

bed. Spatial distributions of clay-silt-sand content in the west bench area are shown in Figure E-13. No spatial pattern is evident in the raw data shown on this figure. Similar displays of the data for the navigation channel and east bench area are provided in Figures E-14 and E-15, respectively.

E.3 GEOCHRONOLOGY ANALYSIS

Estimation of net sedimentation rates using ^{210}Pb data relies on determination of the unsupported fraction of the total ^{210}Pb activity, also referred to as excess ^{210}Pb . The unsupported fraction ($^{210}\text{Pb}_u$) is estimated as follows:

$$^{210}\text{Pb}_u = ^{210}\text{Pb}_T - ^{210}\text{Pb}_s \quad (\text{Equation E-1})$$

where $^{210}\text{Pb}_T$ is the total ^{210}Pb activity reported by the laboratory in the sediment samples, and $^{210}\text{Pb}_s$ is the supported ^{210}Pb activity derived from natural decay in sediments. Unsupported $^{210}\text{Pb}_u$ activities are computed by subtracting the average supported $^{210}\text{Pb}_s$ activity from the total $^{210}\text{Pb}_T$ activities throughout the sediment column, as per Equation E-1. The unsupported $^{210}\text{Pb}_u$ activities are transformed to natural log space (i.e., $\ln [^{210}\text{Pb}_u]$) and plotted as a function of core depth. A linear regression of $\ln(^{210}\text{Pb}_u)$ versus core depth is performed, and the slope of this line (m) is used to estimate the average net sedimentation rate (PbR with units of cm/yr):

$$\text{PbR} = -0.0311/\text{m} \quad (\text{Equation E-2})$$

This approach, however, requires knowledge of the supported ($^{210}\text{Pb}_s$) activity in the sediments, which is not the case for this study. Therefore, to account for this uncertainty in the supported ($^{210}\text{Pb}_s$) activity, an analysis was performed to determine the best estimate of the net sedimentation rate for each core based on varying assumptions regarding unsupported $^{210}\text{Pb}_u$ activities in the LDW sediments. This analysis was performed independently for each of the eight cores with interpretable $^{210}\text{Pb}_T$ profiles as follows:

1. A range of supported ($^{210}\text{Pb}_s$) activities is determined for each core by computing the upper and lower 95% CIs around the average $^{210}\text{Pb}_T$ activity in the deeper sediments of each core, which are assumed to contain background levels of $^{210}\text{Pb}_T$ (see top panels in Figures E-16 through E-23).
2. Unsupported $^{210}\text{Pb}_u$ activities are computed by subtracting the lower 95% CI value for the supported $^{210}\text{Pb}_s$ activity from the total $^{210}\text{Pb}_T$ activities throughout the sediment column, as in Equation E-1. This step is repeated assuming various supported $^{210}\text{Pb}_s$ activities within the limits of the lower and upper 95% CIs computed in Step 1, yielding approximately eight to ten unsupported $^{210}\text{Pb}_u$ activity profiles for each core.
3. Each unsupported $^{210}\text{Pb}_u$ activity profile is transformed to natural log space (i.e., $\ln [^{210}\text{Pb}_u]$) and plotted as a function of core depth. A linear regression of $\ln(^{210}\text{Pb}_u)$ versus core depth is performed. This step is repeated for each of the unsupported $^{210}\text{Pb}_u$ activity profiles developed in Step 2.

4. The squares of the correlation coefficients (i.e., R^2 values) for each of the regressions are compared. The regression yielding the highest R^2 value is determined to represent the best estimate of the data, and the slope of this line is used to compute the best estimate of the average net sedimentation rate (as per Equation E-2; see bottom panels in Figures E-16 through E-23).

E.4 IMPLICATIONS FOR SEDIMENT TRANSPORT

As discussed in Section 2.3.3, examination of radionuclide activities in geochronology core samples provides a means for estimating long-term average net sedimentation rates in the LDW. Most cores collected from the bench areas of the LDW exhibit relatively uniform, interpretable ^{137}Cs profiles with depth, suggesting that, overall, these areas are net depositional on annual or decadal time scales. This observation is consistent with the interpretation of the bed property information for these cores (see Section 2.2). However, vertical profiles of physical and chemical properties in the sediments also provide a means of identifying evidence of episodic erosion and deposition events. For some of the LDW cores, the presence of non-detectable activities of ^{137}Cs and variations in the vertical distribution of ^{137}Cs activities, ^{210}Pb activities, TOC and/or total solids content are indications that episodic erosion and deposition may be occurring on a local scale. As a result, these features are investigated further in an attempt to interpret the sediment transport regime at each core location. A core-by-core discussion is provided below.

E.4.1 Core Sg-1a

This core was collected from a west bench area of the LDW in the vicinity of RM 0.2. Evaluation of the ^{137}Cs data suggest average net sedimentation rates of 0.9 to 1.3 cm/yr (based on both 1963 and 1954 ^{137}Cs markers). These rates indicate that this region is net depositional on annual to decadal time scales. Two elevated ^{137}Cs measurements (i.e., relative to activities in adjacent segments) located about 10 and 25 cm below the sediment surface are potential indications that this area may have experienced episodic erosion and/or deposition. However, the overlapping error bars (which represent 95% CI around the reported measurement) indicate that these two elevated ^{137}Cs measurements are not statistically different from the ^{137}Cs concentrations measured in adjacent segments. The TOC and total solids levels in this core are uniform with depth, and exhibit no clear signs of episodic erosion/deposition events (Figure 2-13).

E.4.2 Core Sg-2

This core was collected from the shallow channel to the west of Kellogg Island. Cesium-137 activities in this core exhibit a typical vertical profile (i.e., ^{137}Cs activities initially increase with sediment depth, peak at depth, and decline to non-detectable below the peak; Figure 2-14). However, ^{137}Cs activities are relatively low throughout the entire sediment column (ranging from non-detect to 0.18 pCi/g dw) and no distinct ^{137}Cs peak is evident. The first presence of detectable ^{137}Cs is found

approximately 25 cm below the sediment surface, indicating that net sedimentation in this area ranges from 0.5 to 0.6 cm/yr on average. These rates are similar to those determined from the ^{210}Pb data (0.5 cm/yr, 0.4 to 1.1 cm/yr). The presence of the 1954 marker in the absence of a ^{137}Cs peak suggests that either the true ^{137}Cs peak resides within a sediment segment that was not analyzed during this study (i.e., in sediments located between those analyzed for ^{137}Cs), or that this area experienced an episodic erosion event that removed sediments containing the ^{137}Cs peak from this area. Although some variation in TOC and total solids with depth is evident, the profiles do not provide any clear indications of episodic erosion/deposition events.

E.4.3 Core Sg-3

This core was collected from the east bench area in the vicinity of RM 1.15. Cesium-137 activities peak about 80-81 cm below the sediment surface, indicating an average net sedimentation rate of 1.9 to 2.1 cm/yr for this area (Figure 2-15). Net sedimentation rates could not be determined using the 1954 ^{137}Cs marker (possibly resides within a sediment segment that was not analyzed) and ^{210}Pb data (due to un-interpretable profile). Variations in the ^{137}Cs profile in this core could potentially be suggestive of past episodic erosion/deposition events. For example, a secondary ^{137}Cs peak is observed at about 25 cm below the sediment surface. The ^{137}Cs activity at this depth is 0.30 pCi/g dw, which is about 50 to 100% higher than the ^{137}Cs activities immediately above and below this depth and more consistent with peak ^{137}Cs activities in other cores. An apparent increase in ^{137}Cs activities is also evident at depths of about 55 to 60 cm, however, these increases are not statistically different from the ^{137}Cs activities measured in other portions of the sediment column and, thus, do not provide conclusive evidence of a past event(s). Coincident changes in ^{210}Pb , TOC, and total solids content at these depths are not observed.

E.4.4 Core Sg-4

This core was collected from the east bench area in the vicinity of RM 1.4. Cesium-137 activities peak at about 75-76 cm below the sediment surface, indicating an average net sedimentation rate of 1.6 to 2 cm/yr for this area (Figure 2-16). Similar to core Sg-3, net sedimentation rates could not be determined using the 1954 ^{137}Cs marker (buried below deepest analyzed segment) and ^{210}Pb data (due to un-interpretable profile). The ^{137}Cs activities in this core gradually increase from about 0.09 pCi/g dw at the surface to about 0.25 pCi/g dw at a depth of 40 cm. Over the next 10 cm, ^{137}Cs activities alternate between lower (0.16 pCi/g dw) and higher (0.34 pCi/g dw) activities before returning to a relatively constant value of 0.25 pCi/g dw (at 55 and 60 cm). The alternating pattern of high and low ^{137}Cs suggests that this core was subjected to disturbance as a result of an episodic event (e.g., deposition of older sediments that were eroded from another area). However, it appears to be limited to a single event or multiple, closely-spaced events in time, because this is the only such occurrence in this core. Coincident changes in ^{210}Pb , TOC, and total solids content at this depth are not observed.

E.4.5 Core Sg-5a

This core was collected from the west bench area in the vicinity of RM 1.9. Evaluation of the ^{137}Cs data suggest average net sedimentation rates of 1.4 to 1.6 cm/yr (based on 1963 ^{137}Cs peak at 60-61 cm). These rates are similar to those determined from the ^{210}Pb data (1.3 cm/yr, 0.7 to 9.3 cm/yr), indicating that this region is net depositional on annual to decadal time scales. The ^{210}Pb , TOC and total solids levels in this core are uniform with depth, and exhibit no clear signs of past episodic erosion/deposition events (Figure 2-17).

E.4.6 Core Sg-6

This core was collected from the west bench area in the vicinity of RM 2.3. Cesium-137 activities in this core peak about 105-106 cm below the sediment surface, indicating an average net sedimentation rate of 2.5 to 2.7 cm/yr for this area (Figure 2-18). This core was collected near the edge of the dredged channel and, thus, the collection of only post-1970 sediments (i.e., only sediments deposited after the 1970s) in this core may indicate that this area was disturbed during past dredging operations.

E.4.7 Core Sg-7

This core was collected from the west bench area in the vicinity of RM 2.7. Cesium-137 activities in this core peak about 80-81 cm below the sediment surface, indicating an average net sedimentation rate of 1.9 to 2.1 cm/yr for this area (Figure 2-19). A secondary ^{137}Cs peak is apparent about 15 cm below the sediment surface, which could be indicative of an episodic event. However, the 95% CI around this ^{137}Cs measurement, as reported by the laboratory, indicate that this measurement is not statistically different from other ^{137}Cs measurements immediately above and below this depth. In addition, the ^{210}Pb , TOC and total solids measurements exhibit relatively uniform levels with depth, suggesting that these sediments have not experienced significant disturbance. Analysis of the ^{210}Pb data yields lower net sedimentation rates relative to the ^{137}Cs data (0.7 cm/yr, 0.5 to 1.1 cm/yr).

E.4.8 Core Sg-8

This core was collected from the east bench area in the vicinity of RM 3.5. Cesium-137 activities in this core are below detectable limits throughout the entire sediment column (Figure 2-20). The cause for this unusual pattern is not known, however, it could be the result of one of two scenarios: 1) this region was depositional until about 1954, when detectable levels of ^{137}Cs are typically first observed, and either erosional or has relatively low deposition thereafter; or 2) the area has been affected by past dredging operations, which removed the historical ^{137}Cs record, followed by significant and rapid deposition of finer grain material. Although some variation is observed in the TOC and total solids measurements with depth, the relative uniformity of the profiles is not indicative of an area that experiences erosion or deposition on a frequent basis.

E.4.9 Core Sg-9

This core was collected from the west bench area in the vicinity of RM 3.6. Cesium-137 activities in this core initially increase with sediment depth, peak at about 0.36 pCi/g dw 15 cm below the sediment surface, and decline to non-detectable levels at about 45 cm (Figure 2-21). The ^{137}Cs peak at about 15 cm suggests average net sedimentation rates of 0.3 to 0.5 cm/yr, which are similar to those determined from the ^{210}Pb data (0.4 cm/yr, 0.2 to >0.4 cm/yr). The first presence of detectable ^{137}Cs at about 40 cm below the sediment surface suggests higher net sedimentation rates of 0.8 to 0.9 cm/yr. The discrepancy between the two estimation methods may be explained by the presence of medium sand (containing non-detectable ^{137}Cs activities) in the top 6 cm of the sediment column, but not in the deeper sediments. The presence of medium sand at the surface and its absence in the deeper sediments of this core suggests that the coarser materials (containing lower ^{137}Cs activities) are not native to this area and were recently deposited in this area.

E.4.10 Core Sg-10

This core was collected from the east bench area in the vicinity of RM 3.6. Cesium-137 activities in this core gradually increase from about 0.1 pCi/g dw at the surface to about 0.3 pCi/g dw at approximately 70 cm below the sediment surface, yielding average net sedimentation rates of 1.6 to 1.8 cm/yr (Figure 2-22). These rates are higher than those determined from the ^{210}Pb data (0.3 cm/yr, 0.2 to 1.0 cm/yr). The ^{210}Pb , TOC and total solids content measurements exhibit relatively uniform levels with depth, suggesting that these sediments have not experienced any significant episodic erosion/deposition events.

E.4.11 Core Sg-11c

This core was collected in shallow waters in the east bench area in the vicinity of RM 3.8. Cesium-137 activities in this core increase from non-detectable levels at the surface to about 0.24 pCi/g dw at depth (Figure 2-24). However, only 36 cm of sediment were retrieved from this location. It is possible that the maximum ^{137}Cs activity of 0.24 pCi/g dw at the bottom of this core represents the 1963 time horizon, but insufficient information exists to make this determination. The un-interpretable ^{137}Cs profile in this core, coupled with the fact that this core was collected from shallow waters, suggests that this area experiences relatively low deposition. Similar to core Sg-9, non-detectable ^{137}Cs activities in the surface sediments are associated with the presence of medium sand. Medium sand is not present in the deeper sediments of this core. The absence of medium sand in the deeper sediments in this core suggests that the coarser materials (containing lower ^{137}Cs activities) are not native to this area and were recently deposited in this area.

E.4.12 Core Sg-11b

This core was collected in shallow waters in the east bench area near RM 3.9. Cesium-137 activities in core Sg-11b exhibit the classic profile (i.e., increase with sediment depth, peak at depth, and decline to non-detectable below the peak), but activities are relatively low (non-detect to 0.16 pCi/g dw; Figure 2-23). As with core Sg-11c, the un-interpretable ¹³⁷Cs profile in this core, coupled with the fact that this core was collected from shallow waters, suggests that this area experiences relatively low deposition. In addition, the presence of medium sand was noted in the surface sediments but not in the deeper sediments, suggesting that the coarser materials (containing lower ¹³⁷Cs activities) are not native to this area and were recently deposited in this area.

E.4.13 Core Sg-12

This core was collected from the west bench area (adjacent to the upper turning basin dredged area) in the vicinity of RM 4.3. Cesium-137 activities in this core are low and remain relatively constant with depth (0.1 to 0.2 pCi/g dw) at levels that are consistent with those in post-1970 sediments (Figure 2-25). In many instances, non-detectable ¹³⁷Cs activities are reported. Lead-210 activities in this core are generally greater than 0.5 pCi/g dw and, in many cases, in excess of 1.0 pCi/g dw; these levels are more consistent with ²¹⁰Pb activities measured in the surface sediments of other cores. These observations, coupled with the fact that this core was collected close to the edge of the dredged channel, suggests that this area was disturbed during past dredging operations and that the sediments in this core were deposited in this area over a relatively short period (either through enhanced deposition or slumping of sediments in this area). TOC and total solids content measured in this core are relatively constant with depth.

E.4.14 Core Sg-13

This core was collected from the east bench area (adjacent to the upper turning basin dredged area) in the vicinity of RM 4.4. Cesium-137 activities in this core peak about 100-101 cm below the sediment surface, indicating an average net sedimentation rate of 2.3 to 2.6 cm/yr for this area (Figure 2-26). A coincident TOC peak is also observed at this depth; the cause for this increase in TOC is not known. TOC and total solids content measurements exhibit relatively uniform levels with depth, suggesting that these sediments have not experienced significant disturbance.

E.5 REFERENCES

Helsel DR, Hirsch RM. 2002. Statistical methods in water resources. Chapter A3, Book 4, Hydrologic analysis and interpretation, Techniques of water-resources investigations of the United States Geological Survey [online]. US Geological Survey, Washington, DC. Updated 2002. Available from: <http://pubs.usgs.gov/twri/twri4a3>.

Interagency Advisory Committee on Water Data (IACWD). 1982. Guidelines for determining flood flow frequency. Bulletin 17B of the Hydrology Subcommittee. U.S. Geological Survey. Reston, VA. 185 pages. Available from: http://water.usgs.gov/osw/bulletin17b/dl_flow.pdf.

LIST OF FIGURES CITED IN APPENDIX E

- Figure E-1. *Frequency of occurrence of high-flow events in the Green River*
- Figure E-2. *Historical freshwater flow rate in the Lower Duwamish Waterway: 1961 through 1964*
- Figure E-3. *Historical freshwater flow rate in the Lower Duwamish Waterway: 1965 through 1968*
- Figure E-4. *Historical freshwater flow rate in the Lower Duwamish Waterway: 1969 through 1972*
- Figure E-5. *Historical freshwater flow rate in the Lower Duwamish Waterway: 1973 through 1976*
- Figure E-6. *Historical freshwater flow rate in the Lower Duwamish Waterway: 1977 through 1980*
- Figure E-7. *Historical freshwater flow rate in the Lower Duwamish Waterway: 1981 through 1984*
- Figure E-8. *Historical freshwater flow rate in the Lower Duwamish Waterway: 1985 through 1988*
- Figure E-9. *Historical freshwater flow rate in the Lower Duwamish Waterway: 1989 through 1992*
- Figure E-10. *Historical freshwater flow rate in the Lower Duwamish Waterway: 1993 through 1996*
- Figure E-11. *Historical freshwater flow rate in the Lower Duwamish Waterway: 1997 through 2000*
- Figure E-12. *Historical freshwater flow rate in the Lower Duwamish Waterway: 2001 through 2004*
- Figure E-13. *Spatial distribution of clay/silt and sand content in surface layer of LDW sediments in west bench area*
- Figure E-14. *Spatial distribution of clay/silt and sand content in surface layer of LDW sediments in navigation channel*
- Figure E-15. *Spatial distribution of clay/silt and sand content in surface layer of LDW sediments in east bench area*
- Figure E-16. *^{210}Pb levels as a function of sediment depth for core Sg-1a*
- Figure E-17. *^{210}Pb levels as a function of sediment depth for core Sg-2*
- Figure E-18. *^{210}Pb levels as a function of sediment depth for core Sg-5a*
- Figure E-19. *^{210}Pb levels as a function of sediment depth for core Sg-6*
- Figure E-20. *^{210}Pb levels as a function of sediment depth for core Sg-7*
- Figure E-21. *^{210}Pb levels as a function of sediment depth for core Sg-9*
- Figure E-22. *^{210}Pb levels as a function of sediment depth for core Sg-10*
- Figure E-23. *^{210}Pb levels as a function of sediment depth for core Sg-13*

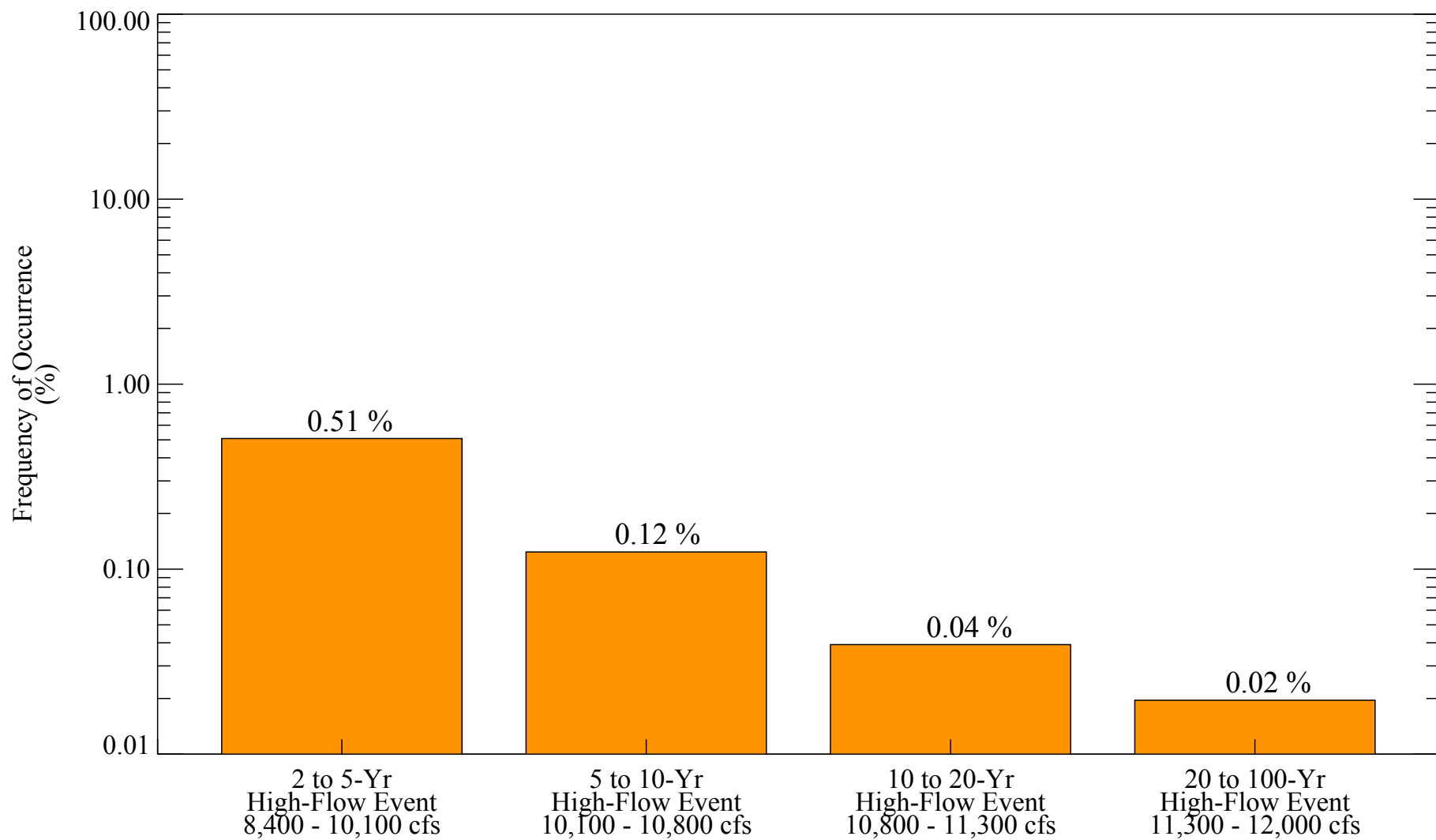


Figure E-1. Frequency of occurrence of high-flow events in the Green River. Period of record is 1961 to 2002. Frequency of occurrence corresponds to number of days during period of record that daily-average flow rate is within a specific high-flow discharge range.

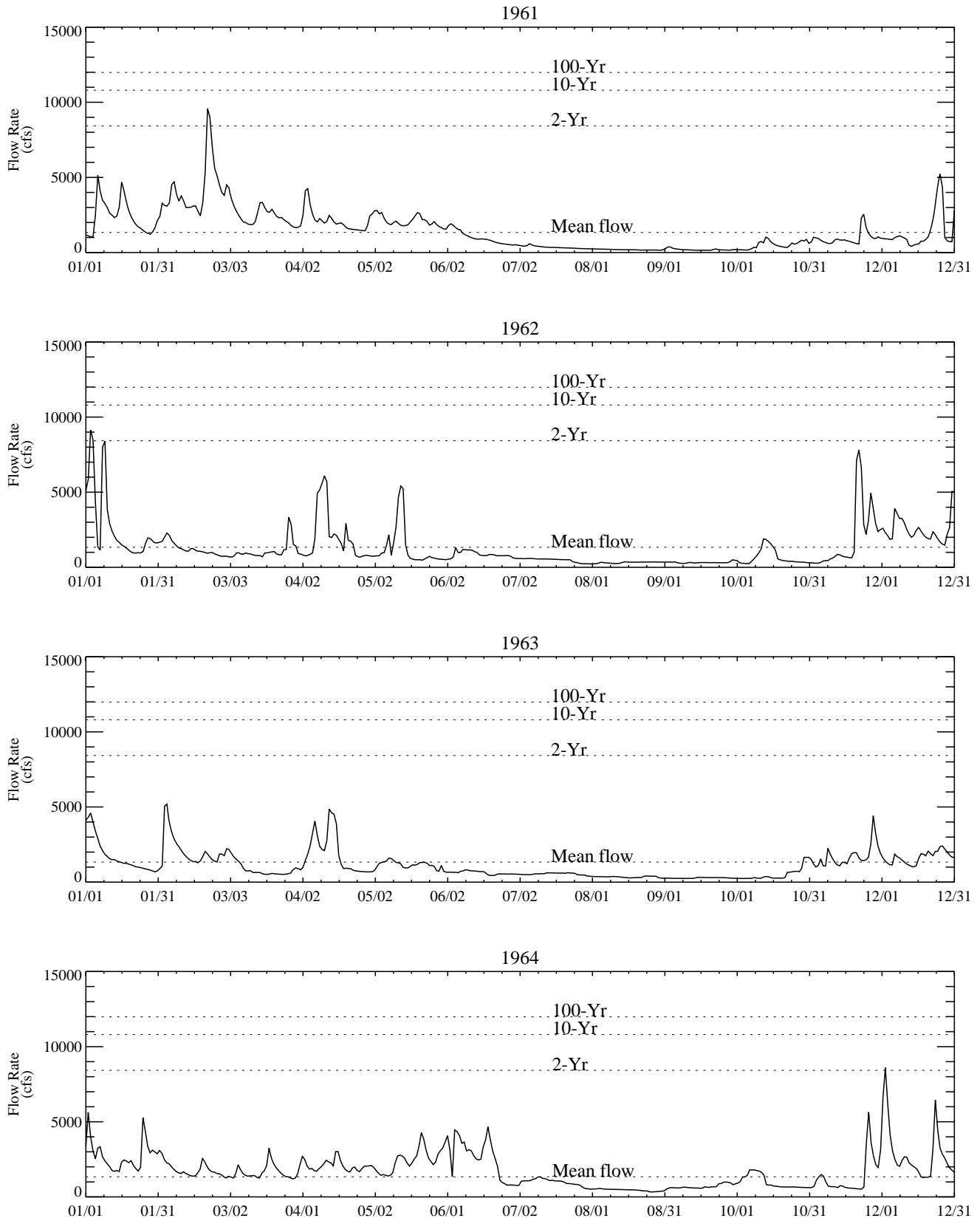


Figure E-2. Historical freshwater flow rate in the Lower Duwamish Waterway: 1961 through 1964.

Daily average discharge measured at USGS gauge at Green River near Auburn, WA.

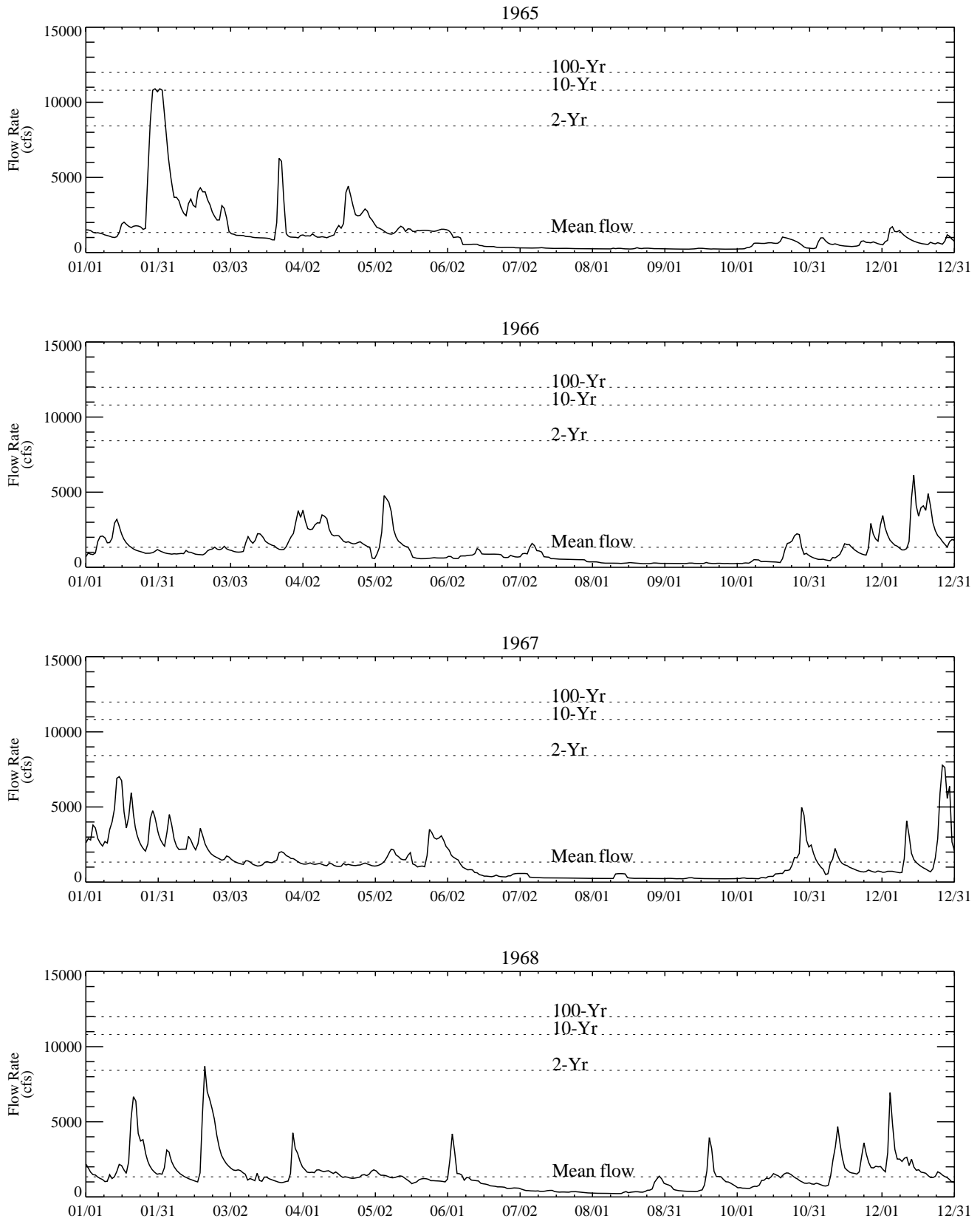


Figure E-3. Historical freshwater flow rate in the Lower Duwamish Waterway: 1965 through 1968.

Daily average discharge measured at USGS gauge at Green River near Auburn, WA.

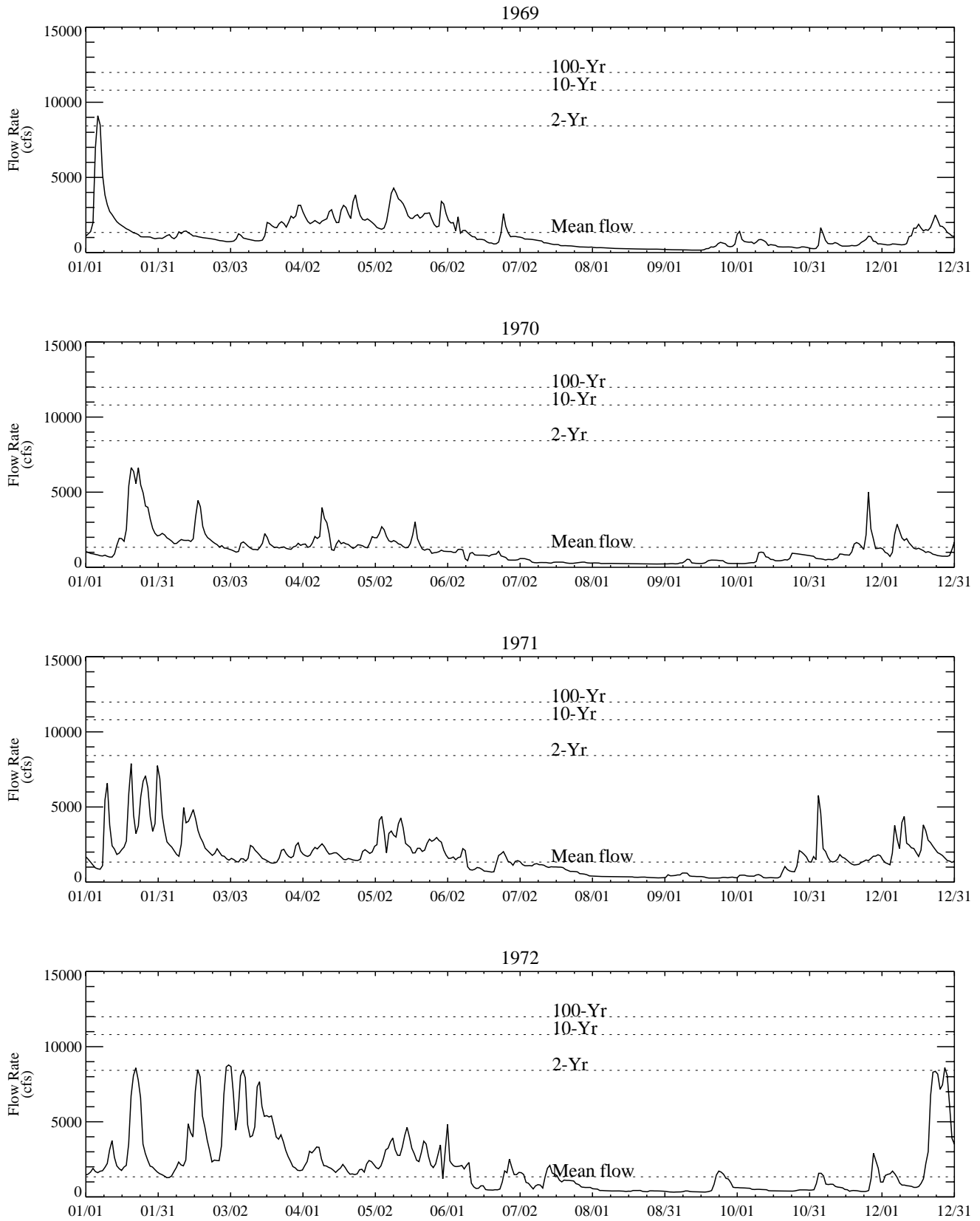


Figure E-4. Historical freshwater flow rate in the Lower Duwamish Waterway: 1969 through 1972.

Daily average discharge measured at USGS gauge at Green River near Auburn, WA.

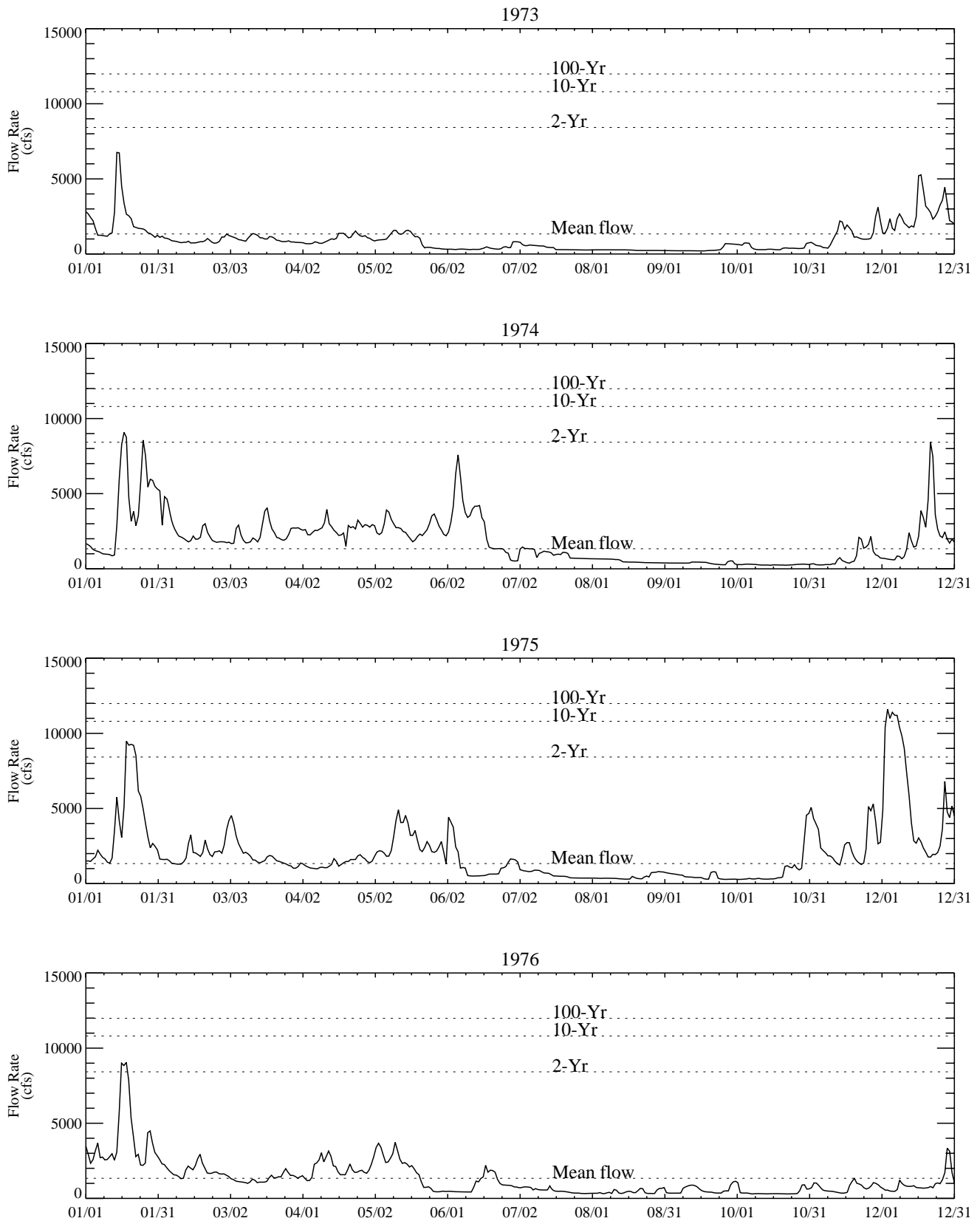


Figure E-5. Historical freshwater flow rate in the Lower Duwamish Waterway: 1973 through 1976.

Daily average discharge measured at USGS gauge at Green River near Auburn, WA.

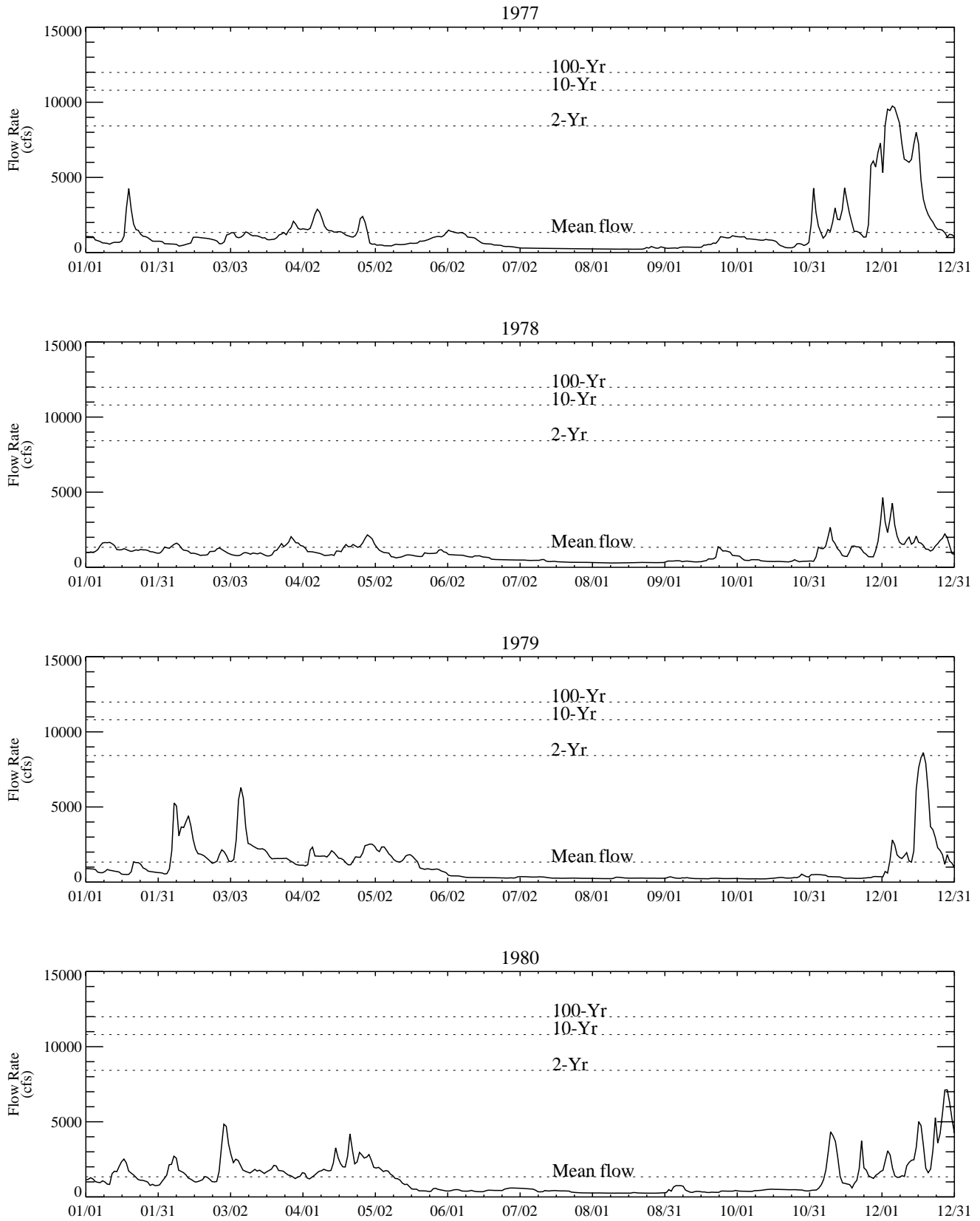


Figure E-6. Historical freshwater flow rate in the Lower Duwamish Waterway: 1977 through 1980.

Daily average discharge measured at USGS gauge at Green River near Auburn, WA.

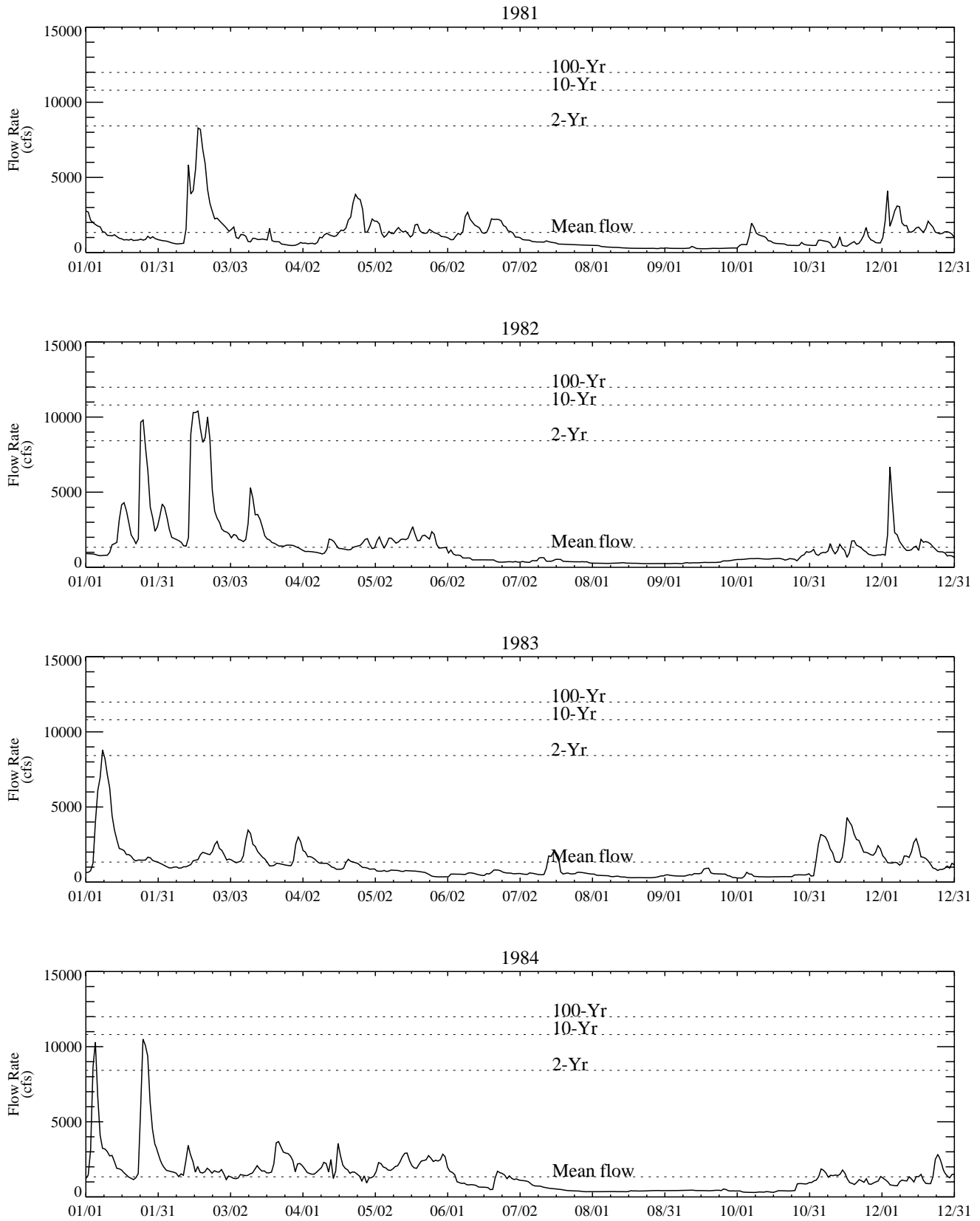


Figure E-7. Historical freshwater flow rate in the Lower Duwamish Waterway: 1981 through 1984.

Daily average discharge measured at USGS gauge at Green River near Auburn, WA.

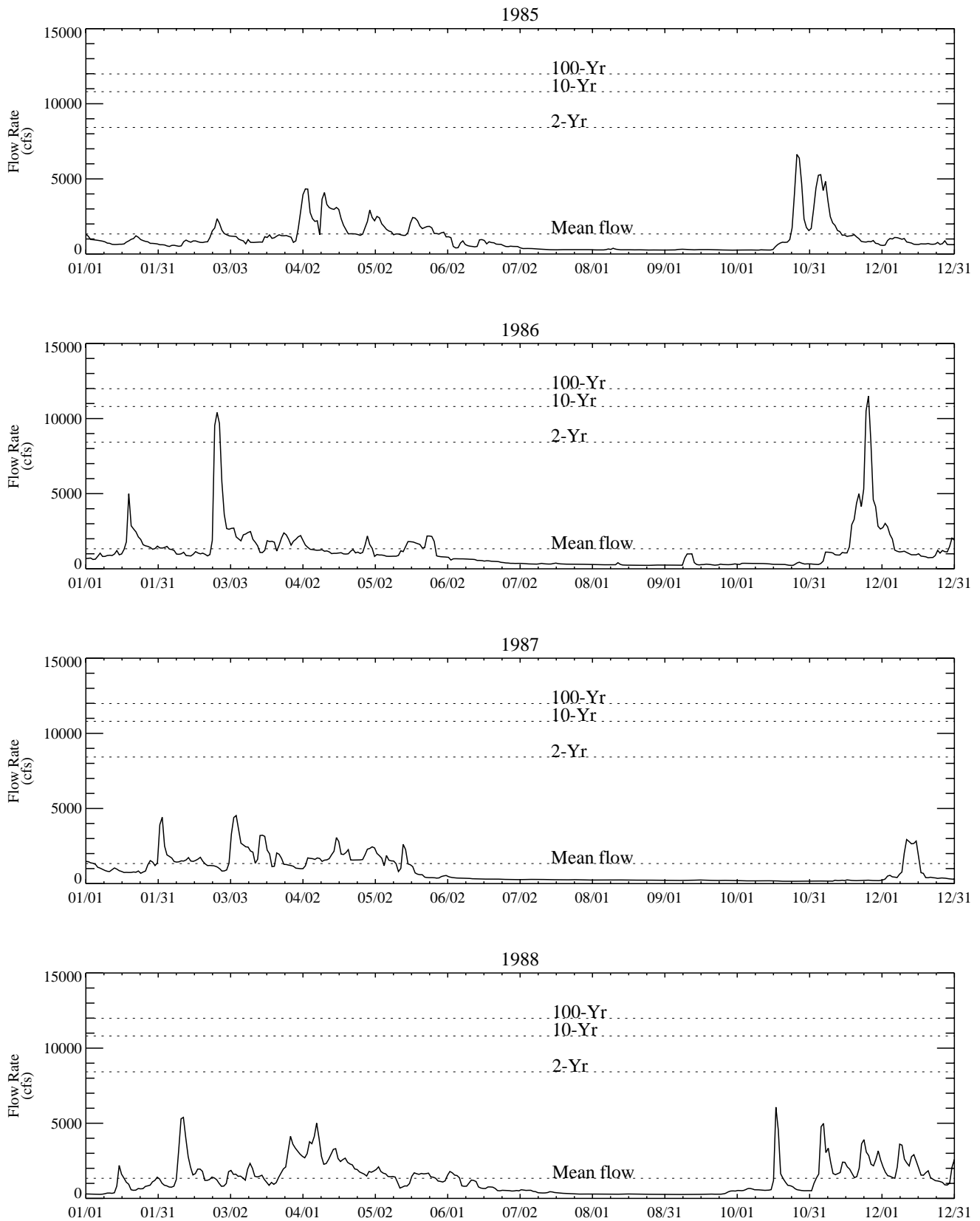


Figure E-8. Historical freshwater flow rate in the Lower Duwamish Waterway: 1985 through 1988.

Daily average discharge measured at USGS gauge at Green River near Auburn, WA.

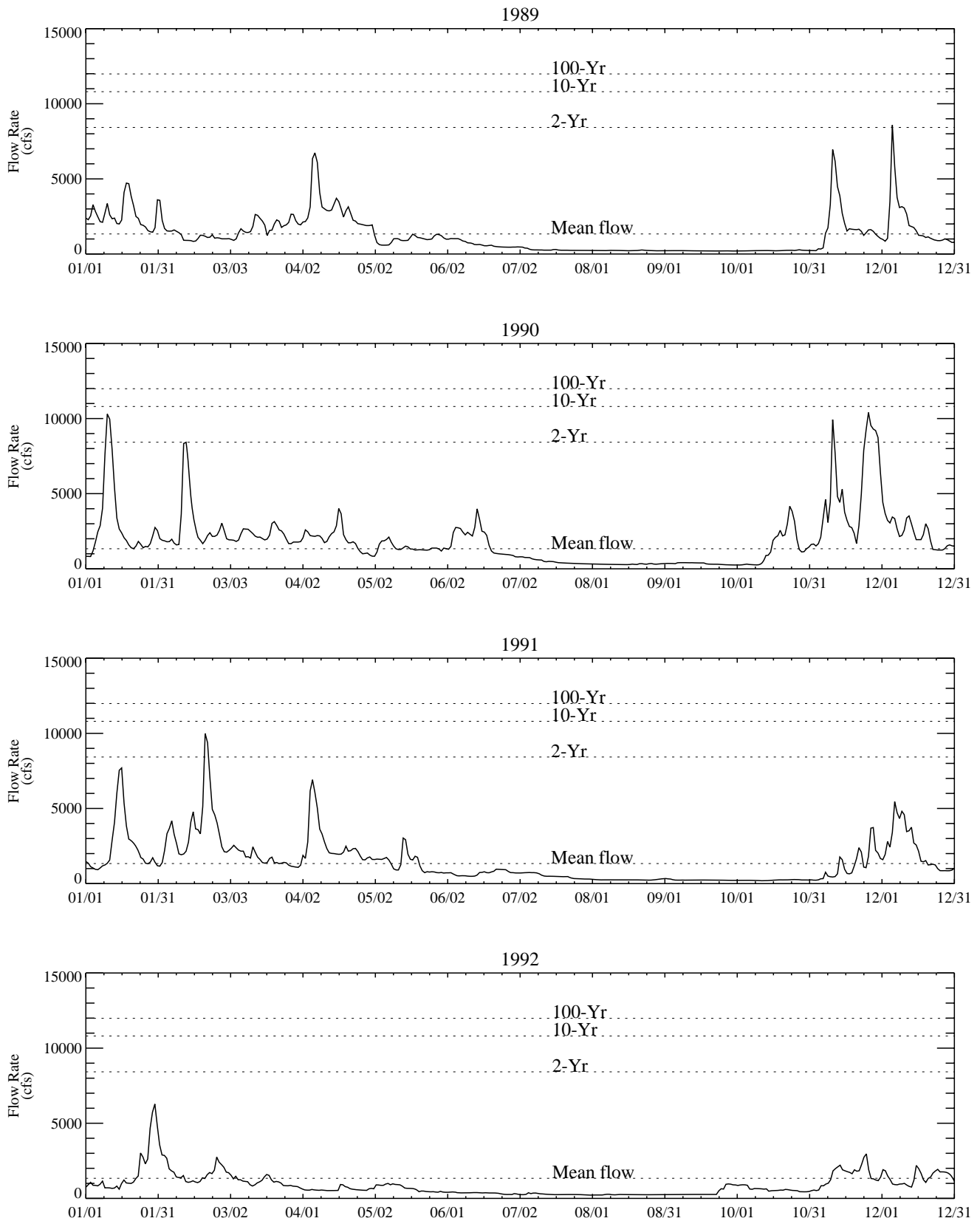


Figure E-9. Historical freshwater flow rate in the Lower Duwamish Waterway: 1989 through 1992.

Daily average discharge measured at USGS gauge at Green River near Auburn, WA.

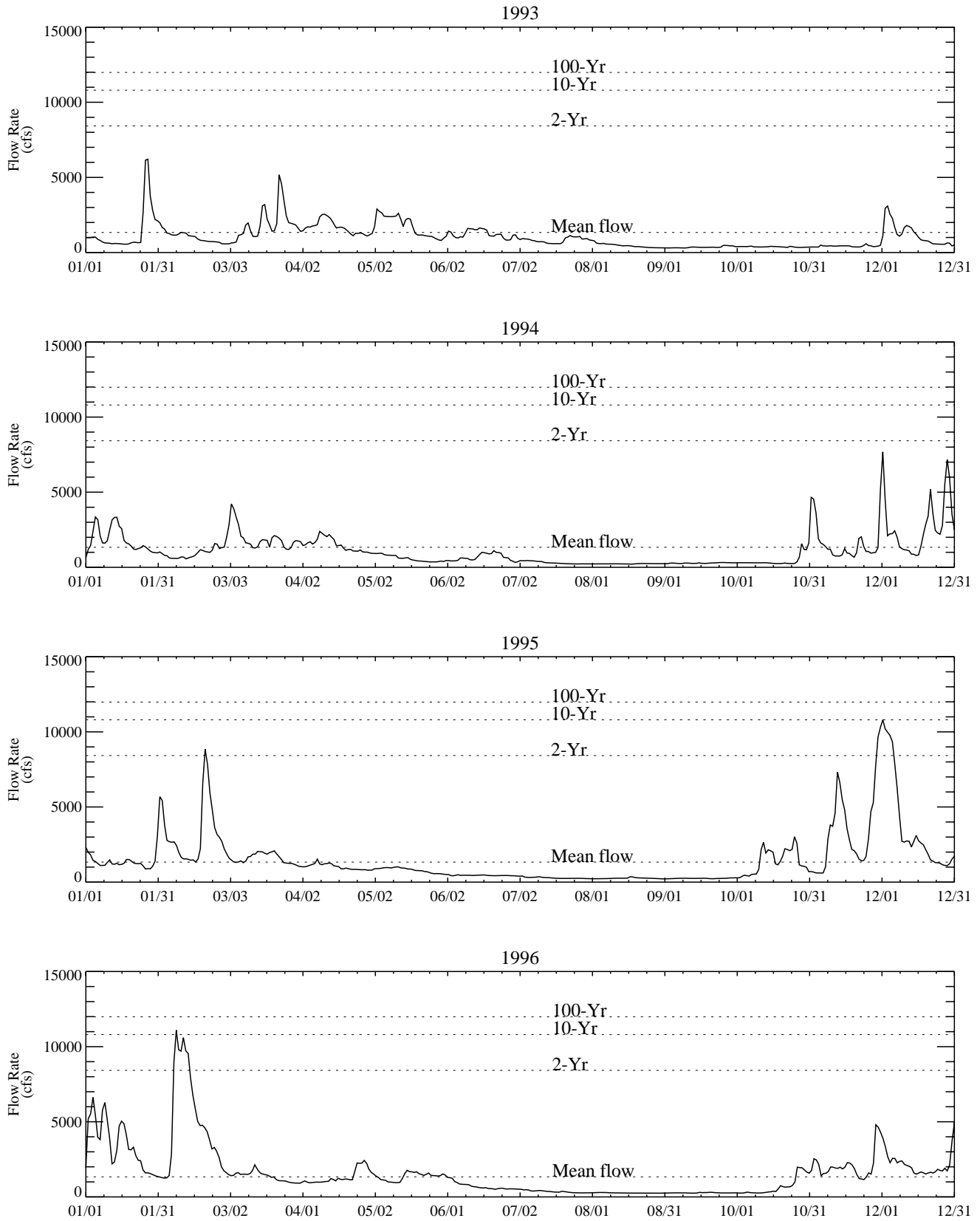


Figure E-10. Historical freshwater flow rate in the Lower Duwamish Waterway: 1993 through 1996.

Daily average discharge measured at USGS gauge at Green River near Auburn, WA.

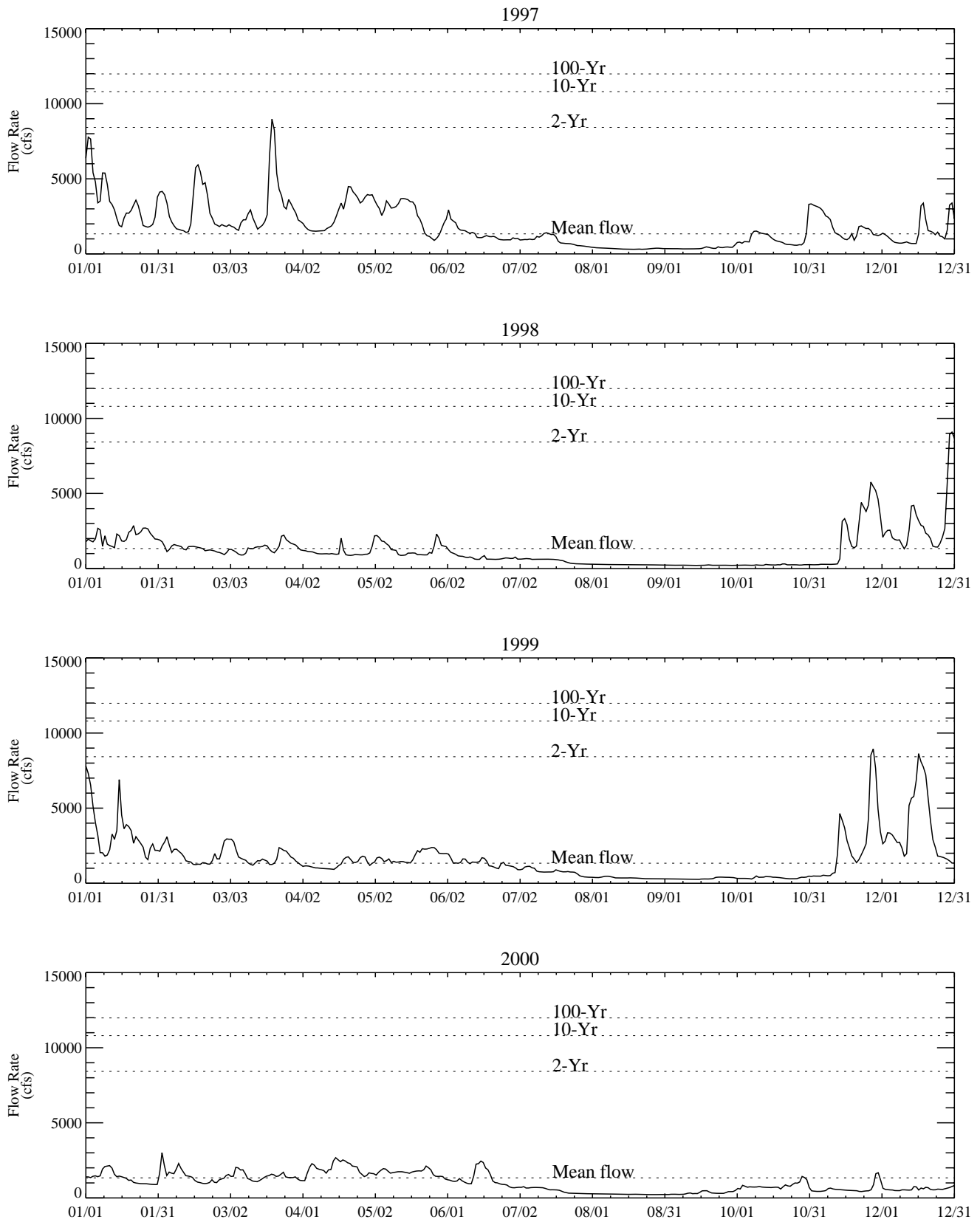


Figure E-11. Historical freshwater flow rate in the Lower Duwamish Waterway: 1997 through 2000.

Daily average discharge measured at USGS gauge at Green River near Auburn, WA.

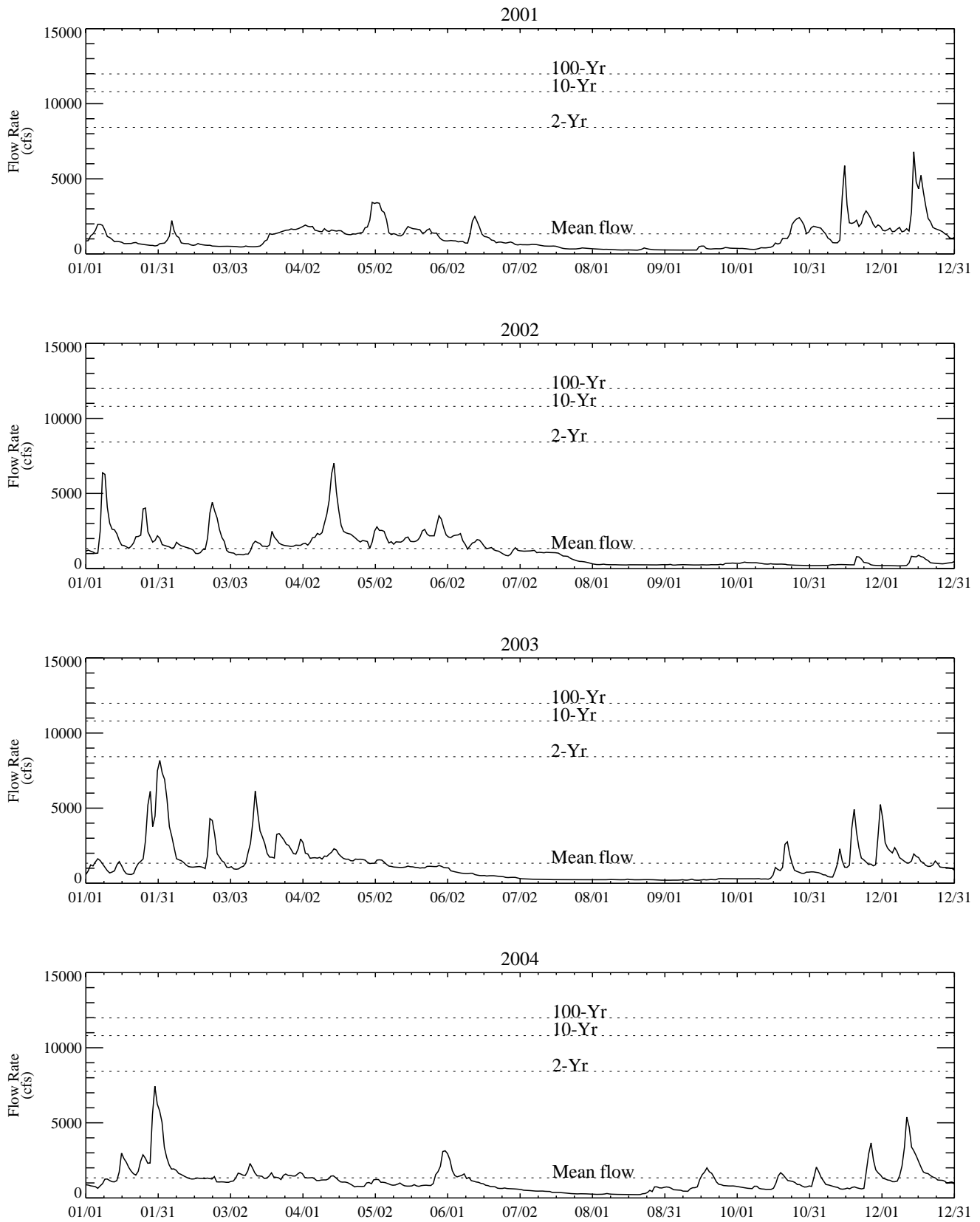


Figure E-12. Historical freshwater flow rate in the Lower Duwamish Waterway: 2001 through 2004.

Daily average discharge measured at USGS gauge at Green River near Auburn, WA.

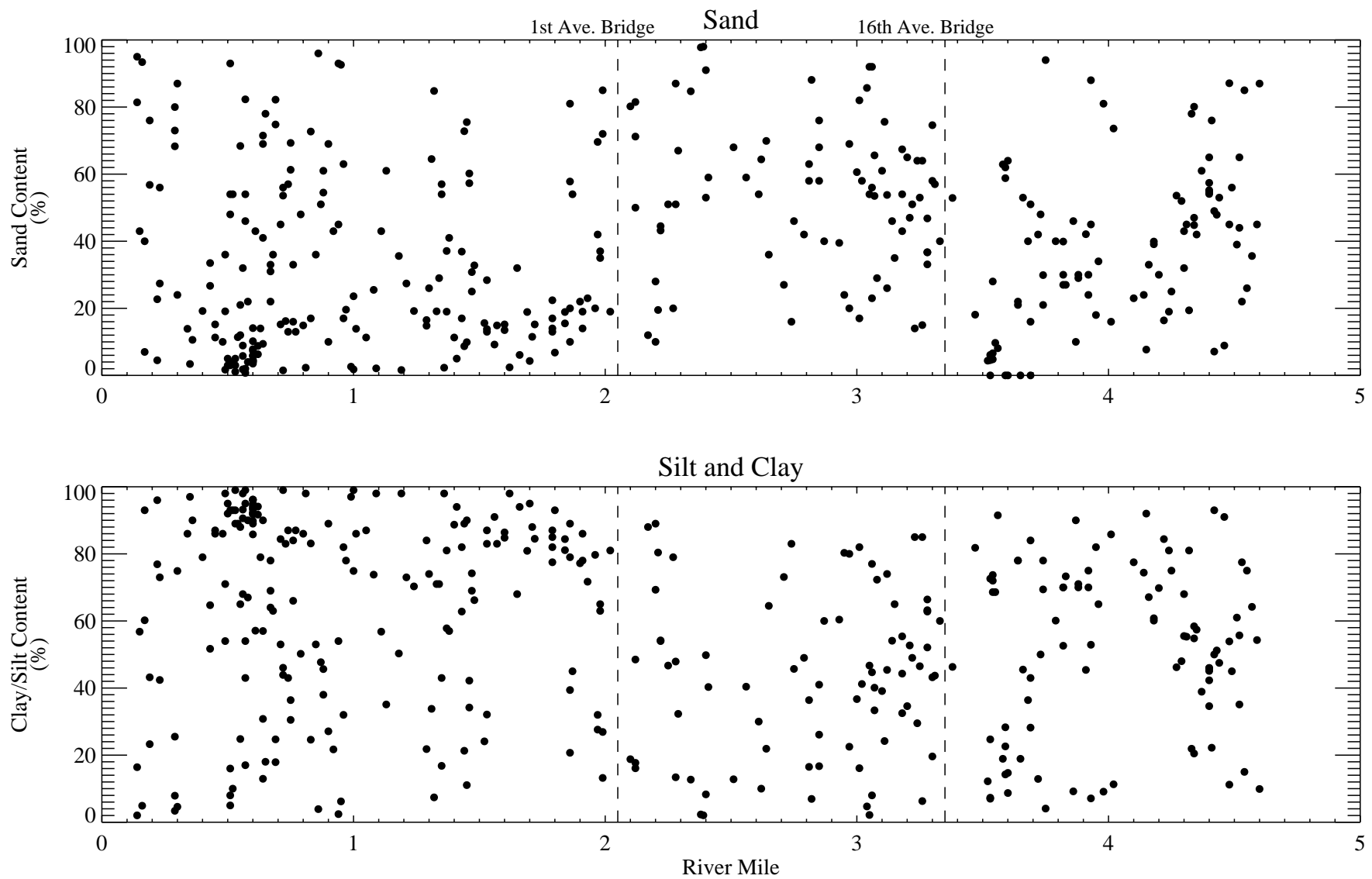


Figure E-13. Spatial distribution of clay/silt and sand content in surface layer of LDW sediments in west bench area.

Grain size data represent historic sampling results between 1991 and 2005.

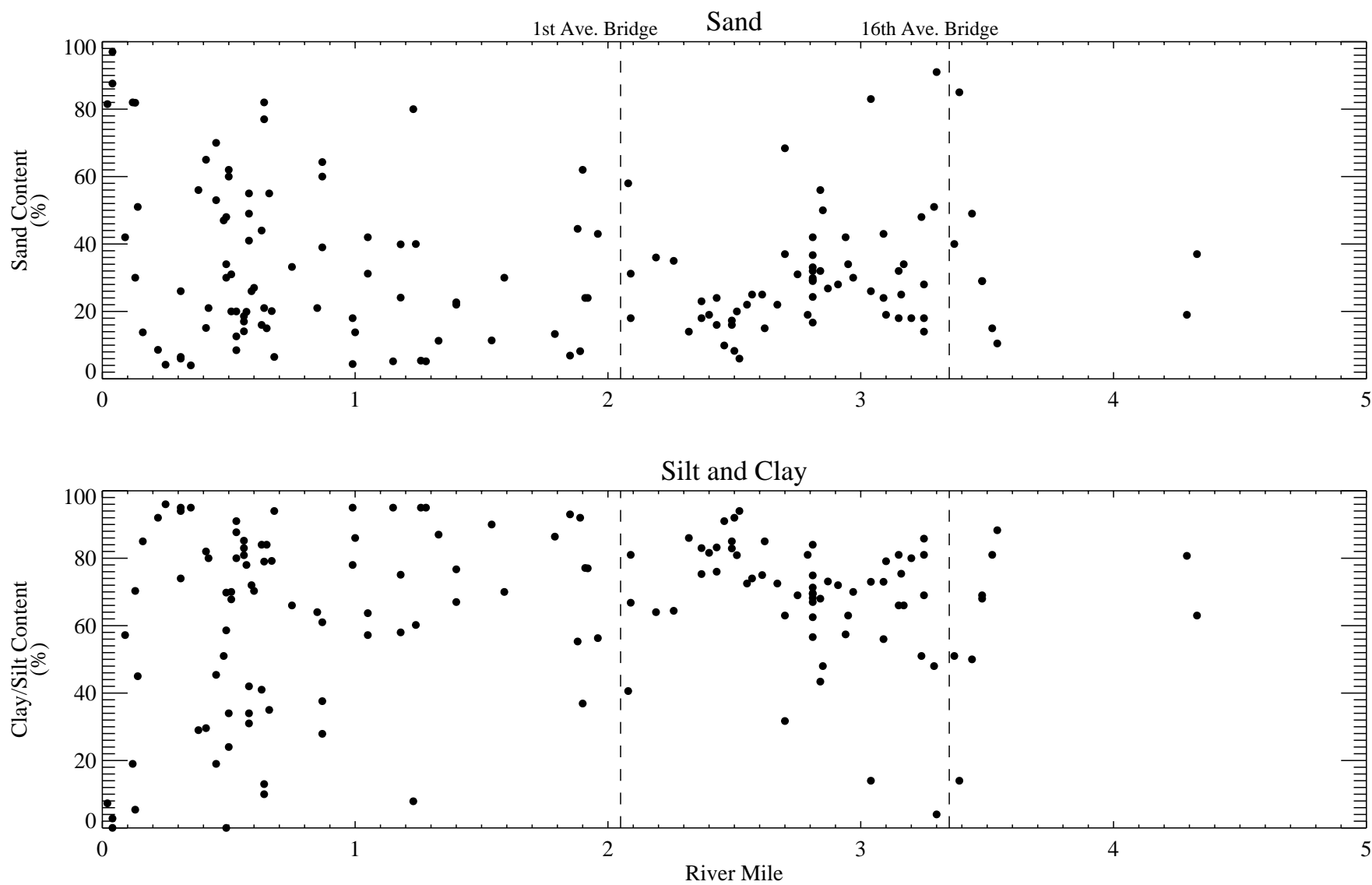


Figure E-14. Spatial distribution of clay/silt and sand content in surface layer of LDW sediments in navigation channel.

Grain size data represent historic sampling results between 1991 and 2005.

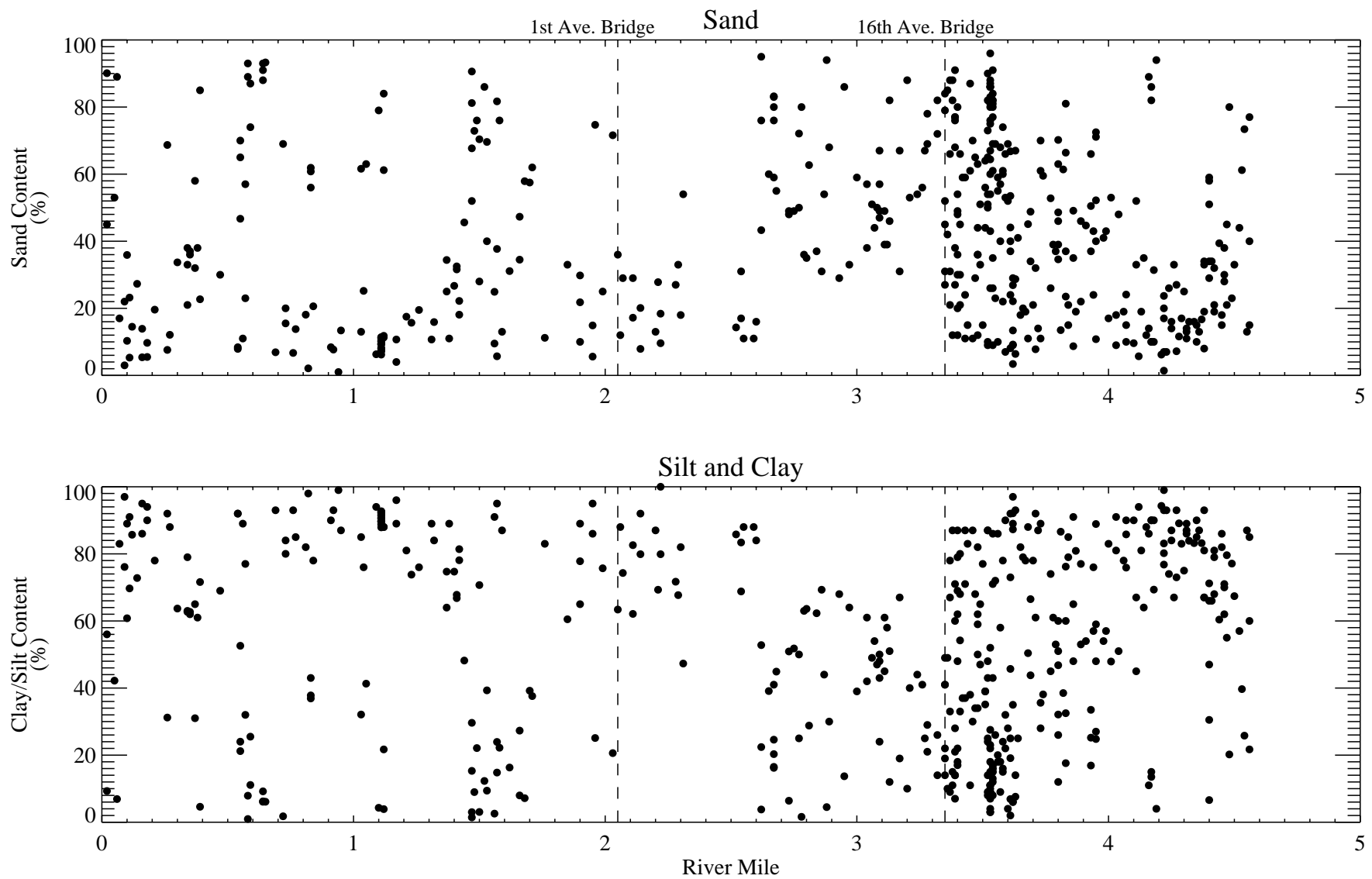


Figure E-15. Spatial distribution of clay/silt and sand content in surface layer of LDW sediments in east bench area.

Grain size data represent historic sampling results between 1991 and 2005.

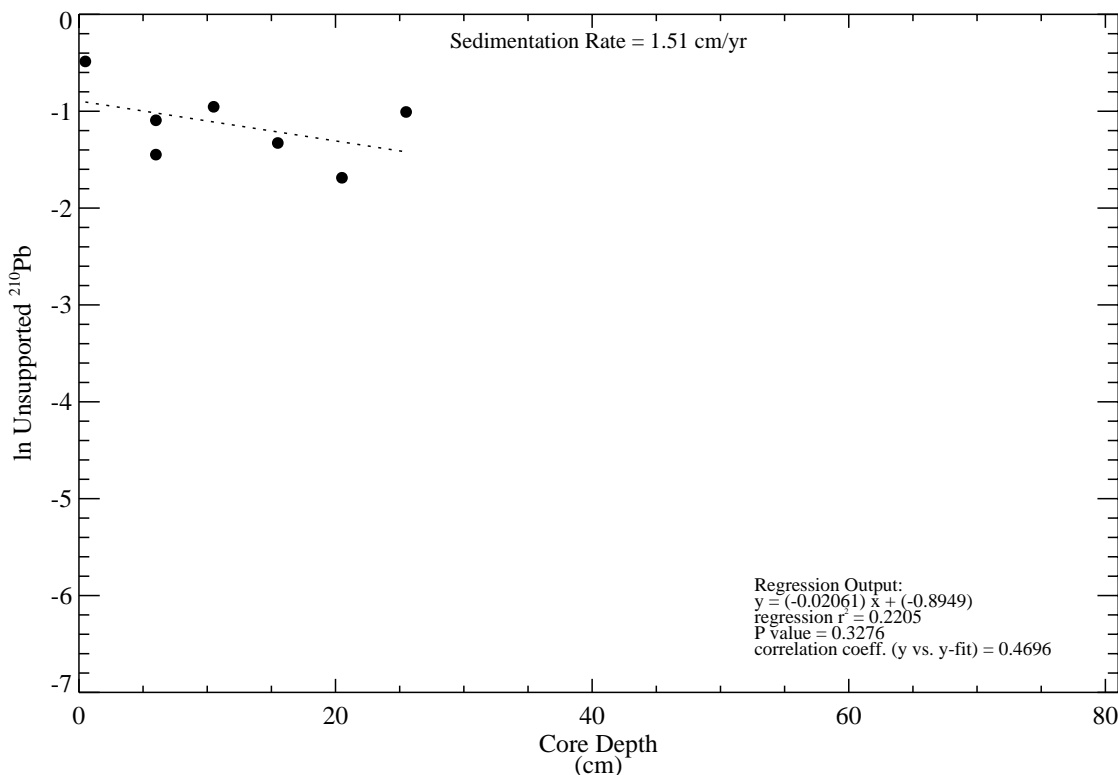
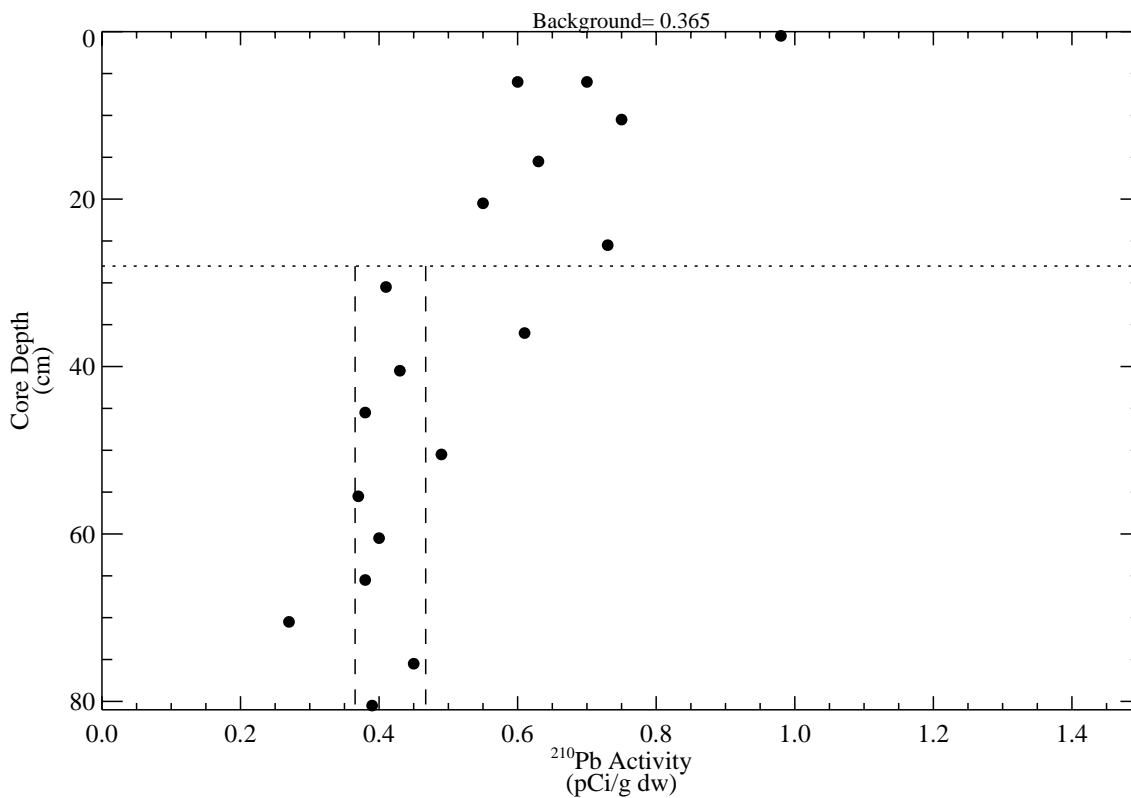


Figure E-16. ^{210}Pb levels as a function of sediment depth for core Sg-1a.

Top panel: vertical distribution of ^{210}Pb activities. Data above dashed horizontal line used in sedimentation rate regression analysis. Vertical lines represent 95% confidence limits of supported ^{210}Pb activities used in regression analysis.

Bottom panel: natural logarithm of unsupported ^{210}Pb activities with depth. Dashed line represents slope of best fit regression.

Orange square symbols represent samples analyzed from archive.

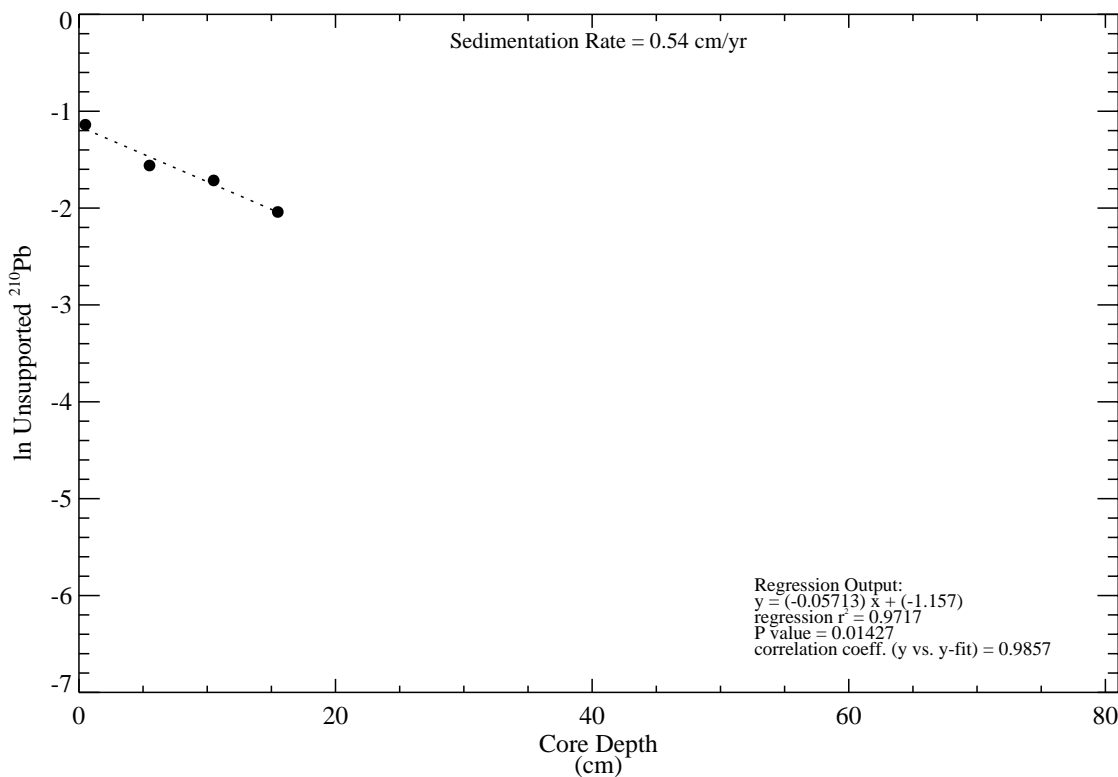
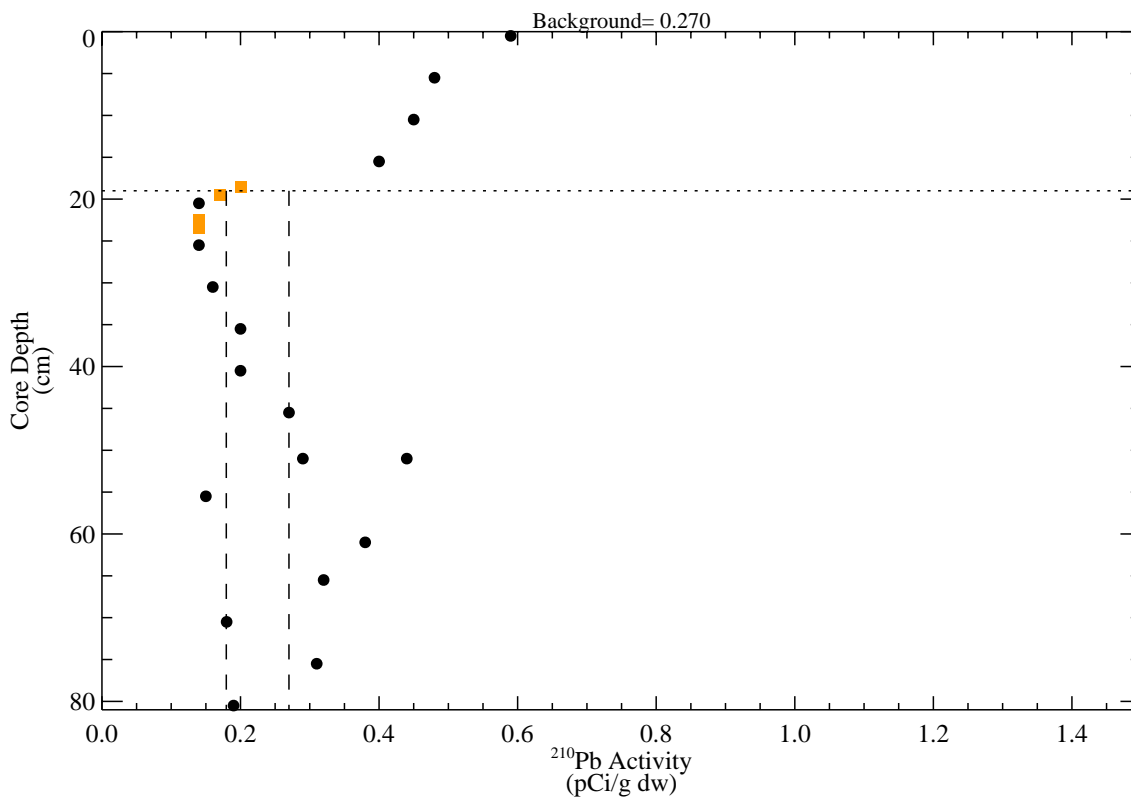


Figure E-17. ²¹⁰Pb levels as a function of sediment depth for core Sg-2.

Top panel: vertical distribution of ²¹⁰Pb activities. Data above dashed horizontal line used in sedimentation rate regression analysis. Vertical lines represent 95% confidence limits of supported ²¹⁰Pb activities used in regression analysis.

Bottom panel: natural logarithm of unsupported ²¹⁰Pb activities with depth. Dashed line represents slope of best fit regression.

Orange square symbols represent samples analyzed from archive.

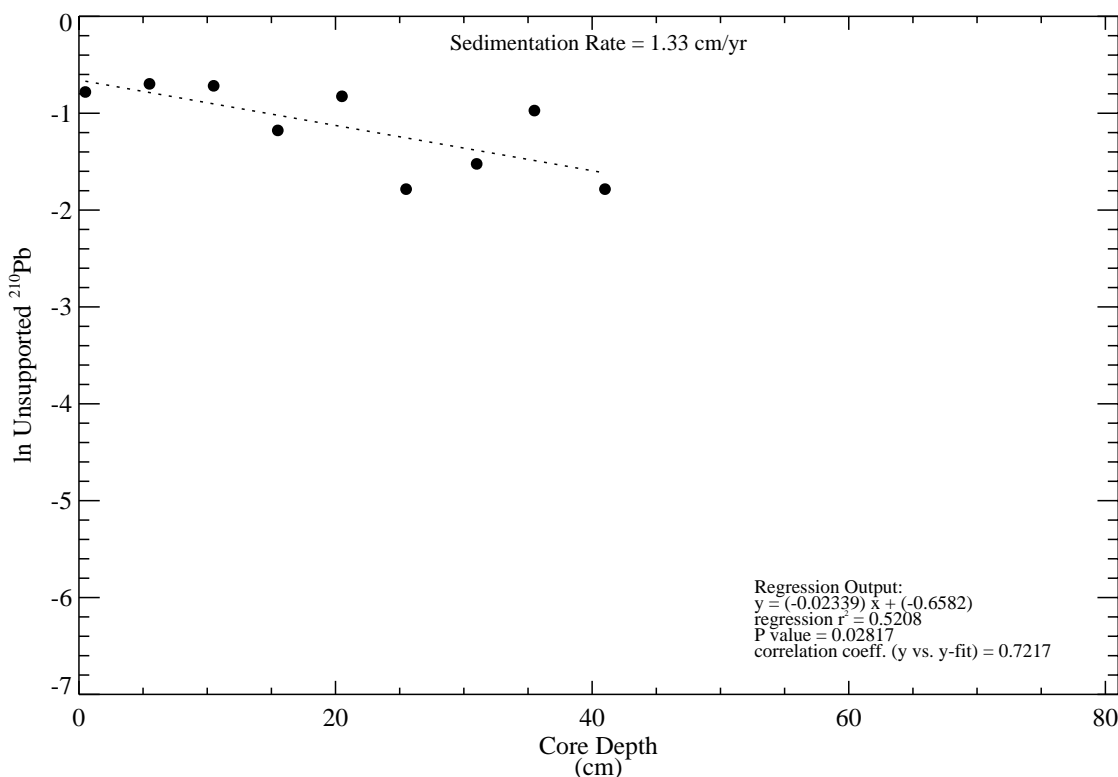
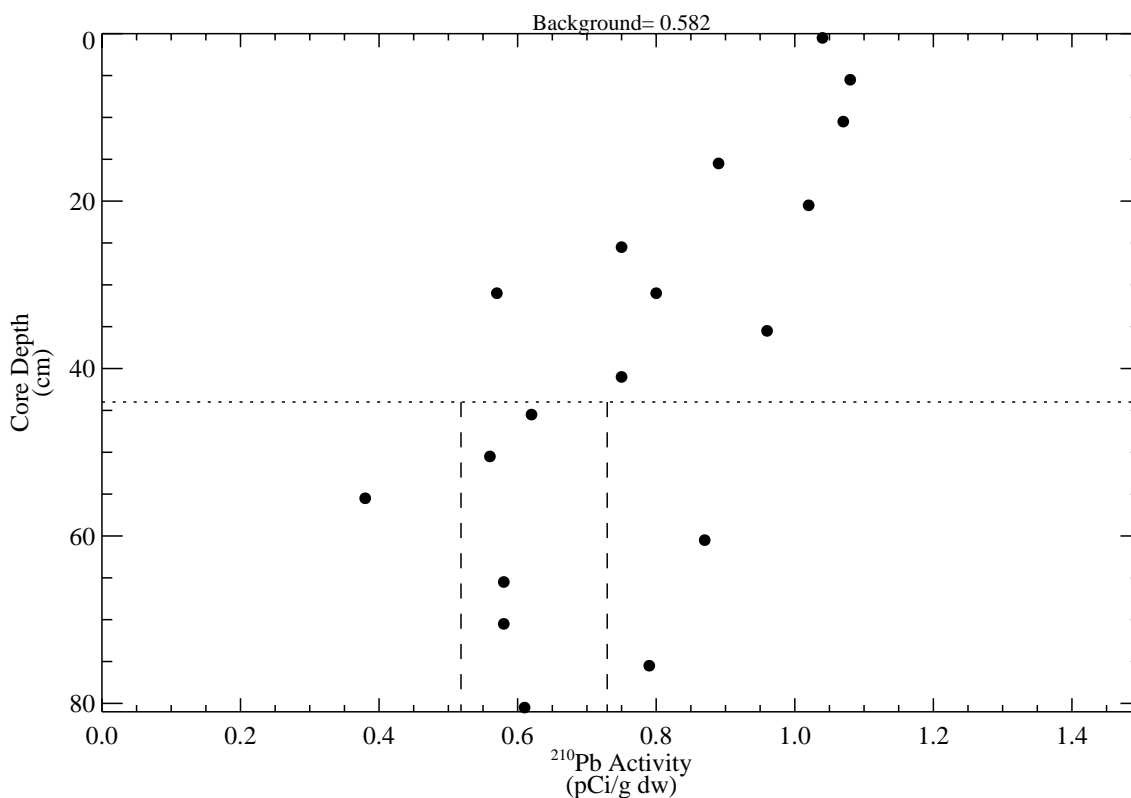


Figure E-18. ^{210}Pb levels as a function of sediment depth for core Sg-5a.

Top panel: vertical distribution of ^{210}Pb activities. Data above dashed horizontal line used in sedimentation rate regression analysis. Vertical lines represent 95% confidence limits of supported ^{210}Pb activities used in regression analysis.

Bottom panel: natural logarithm of unsupported ^{210}Pb activities with depth. Dashed line represents slope of best fit regression.

Orange square symbols represent samples analyzed from archive.

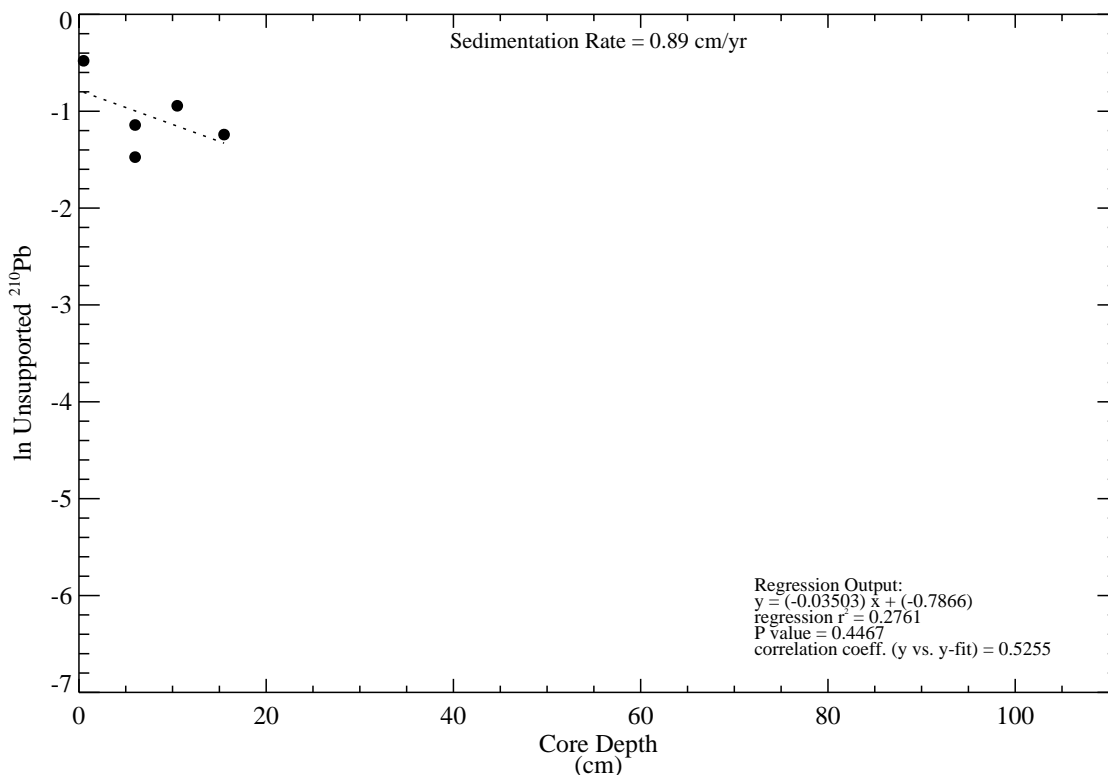
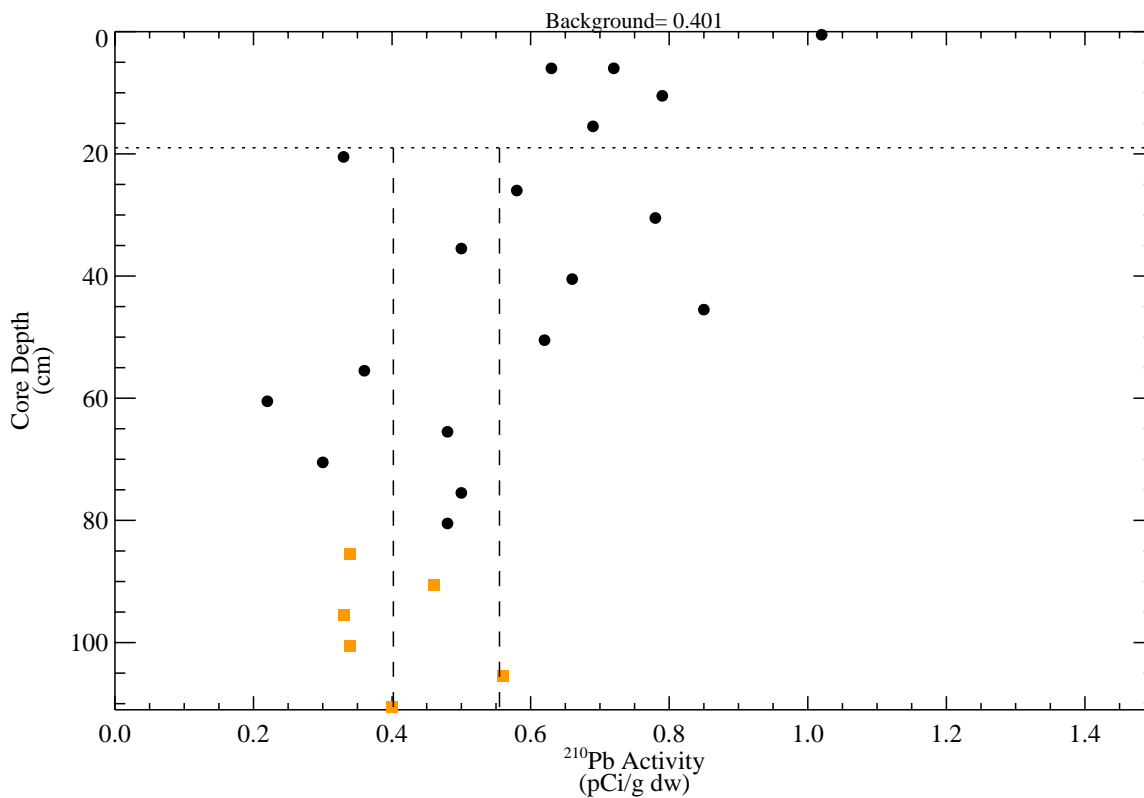


Figure E-19. ²¹⁰Pb levels as a function of sediment depth for core Sg-6.

Top panel: vertical distribution of ²¹⁰Pb activities. Data above dashed horizontal line used in sedimentation rate regression analysis. Vertical lines represent 95% confidence limits of supported ²¹⁰Pb activities used in regression analysis.

Bottom panel: natural logarithm of unsupported ²¹⁰Pb activities with depth. Dashed line represents slope of best fit regression.

Orange square symbols represent samples analyzed from archive.

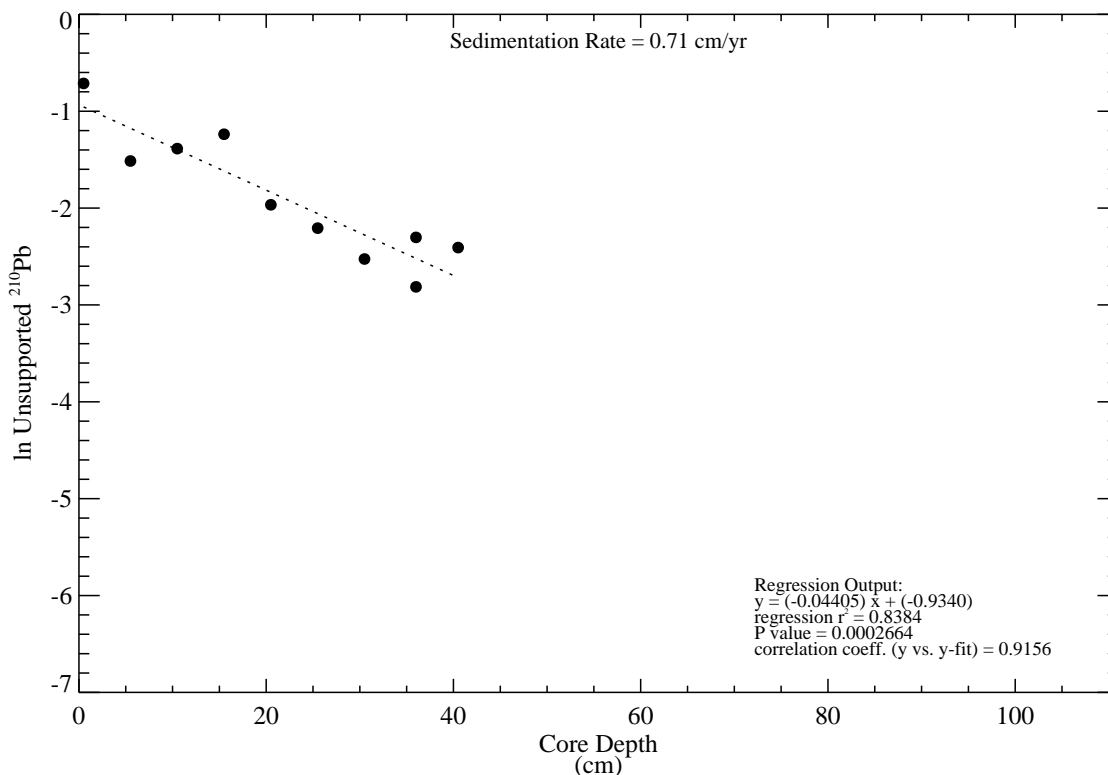
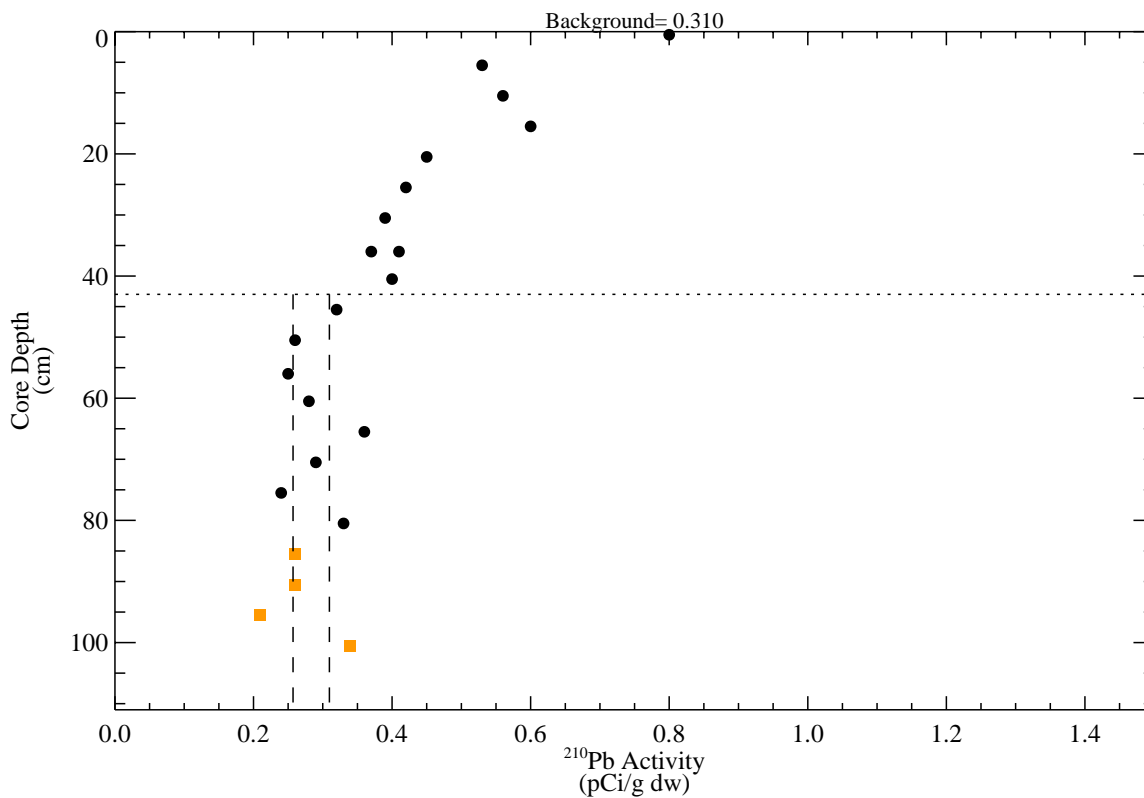


Figure E-20. ^{210}Pb levels as a function of sediment depth for core Sg-7.

Top panel: vertical distribution of ^{210}Pb activities. Data above dashed horizontal line used in sedimentation rate regression analysis. Vertical lines represent 95% confidence limits of supported ^{210}Pb activities used in regression analysis.

Bottom panel: natural logarithm of unsupported ^{210}Pb activities with depth. Dashed line represents slope of best fit regression.

Orange square symbols represent samples analyzed from archive.

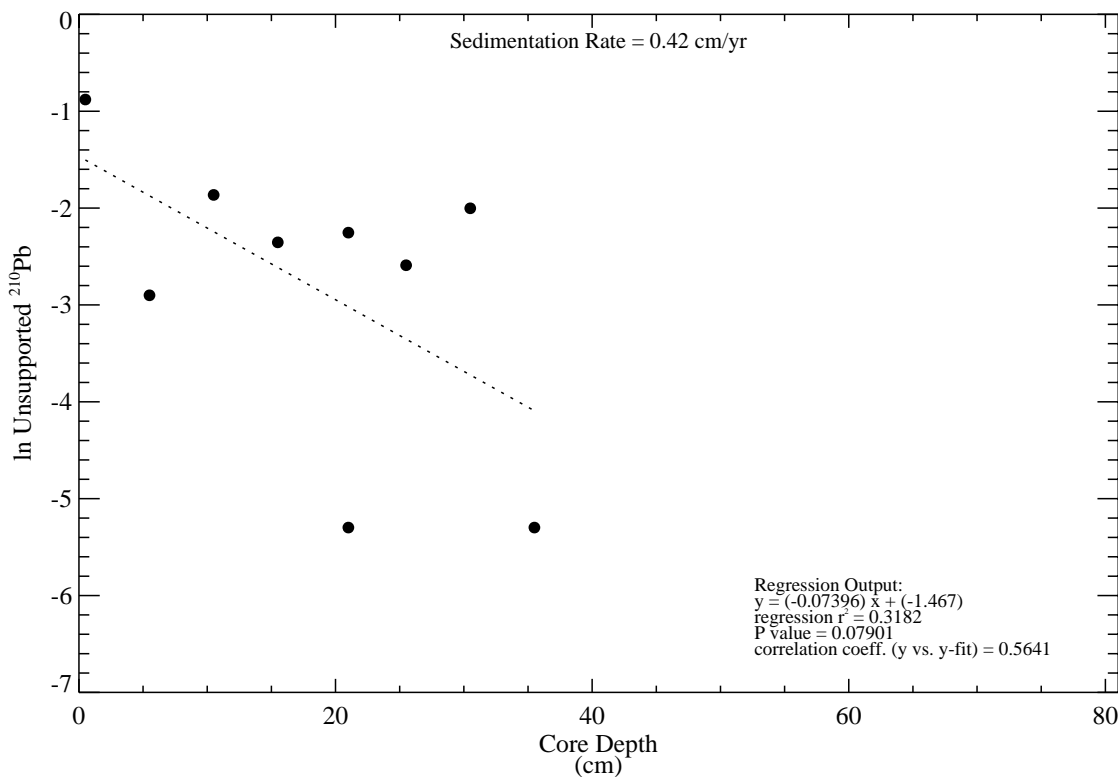
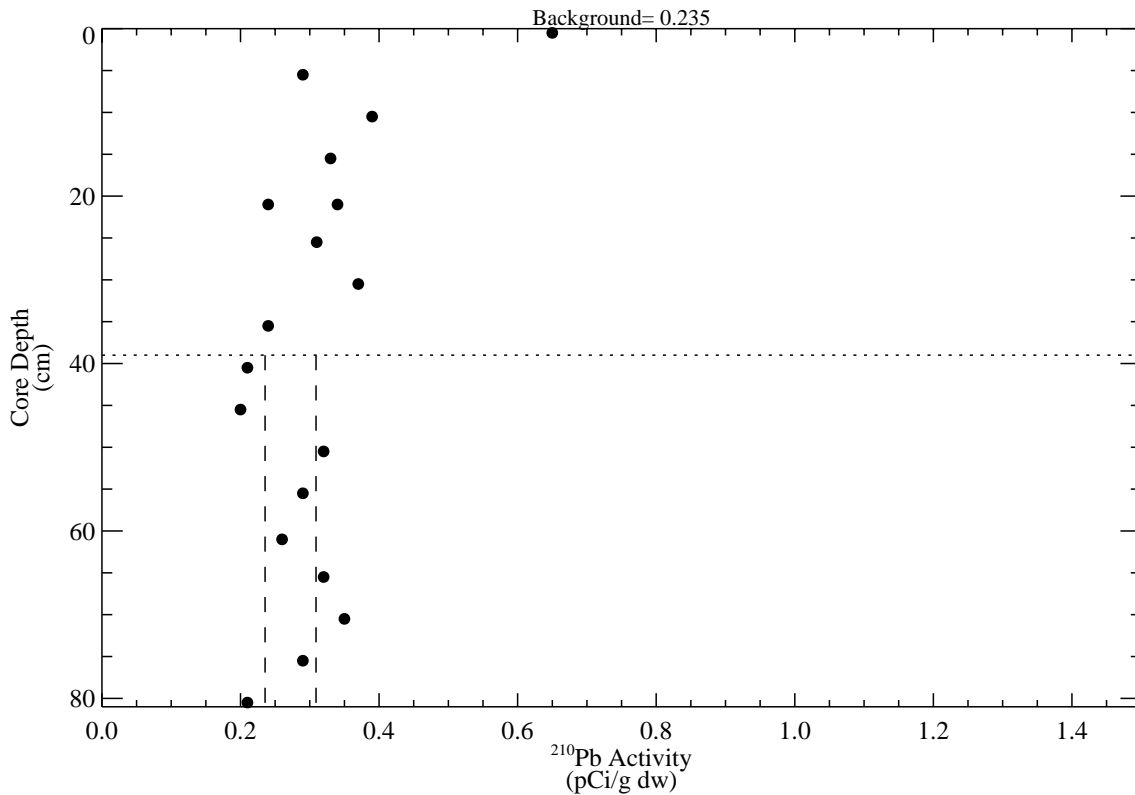


Figure E-21. ²¹⁰Pb levels as a function of sediment depth for core Sg-9.

Top panel: vertical distribution of ²¹⁰Pb activities. Data above dashed horizontal line used in sedimentation rate regression analysis. Vertical lines represent 95% confidence limits of supported ²¹⁰Pb activities used in regression analysis.

Bottom panel: natural logarithm of unsupported ²¹⁰Pb activities with depth. Dashed line represents slope of best fit regression.

Orange square symbols represent samples analyzed from archive.

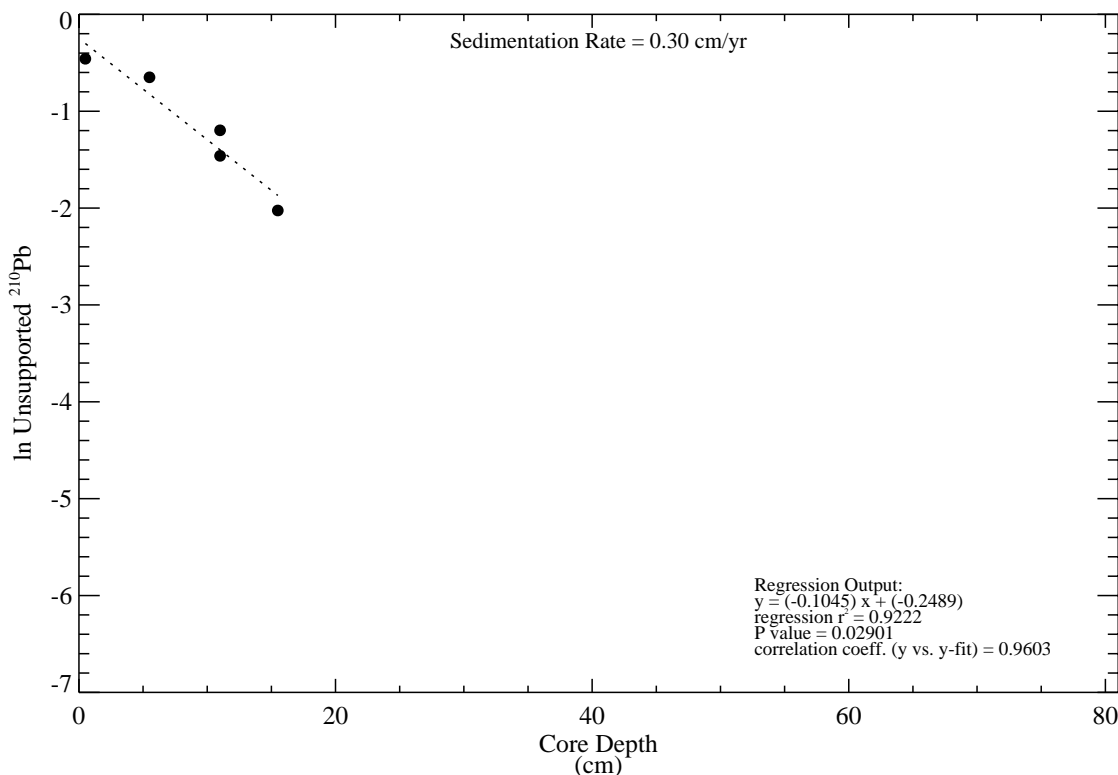
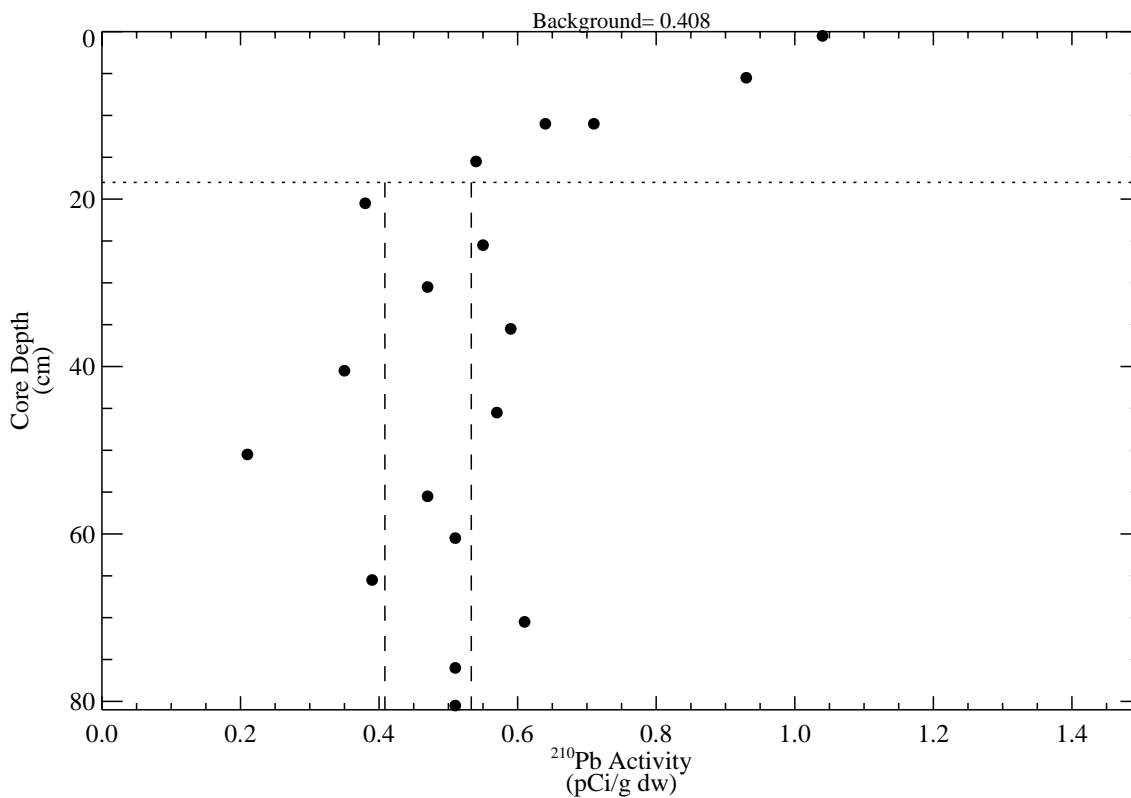


Figure E-22. ^{210}Pb levels as a function of sediment depth for core Sg-10.

Top panel: vertical distribution of ^{210}Pb activities. Data above dashed horizontal line used in sedimentation rate regression analysis. Vertical lines represent 95% confidence limits of supported ^{210}Pb activities used in regression analysis.

Bottom panel: natural logarithm of unsupported ^{210}Pb activities with depth. Dashed line represents slope of best fit regression.

Orange square symbols represent samples analyzed from archive.

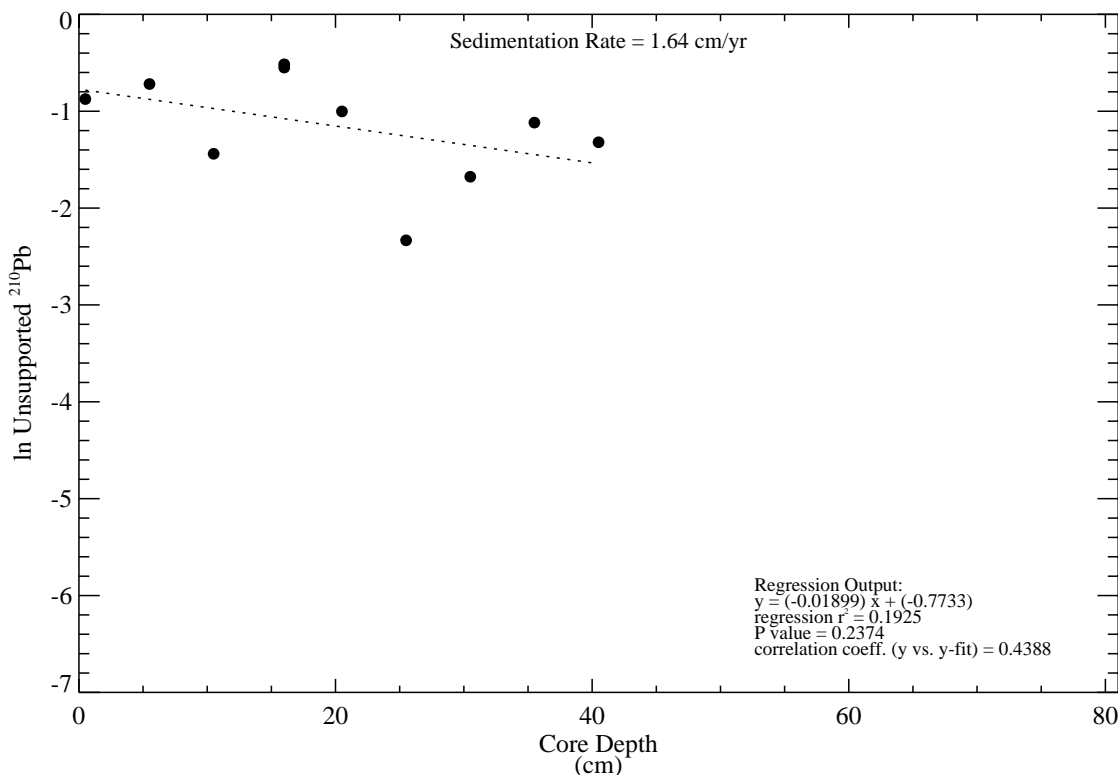
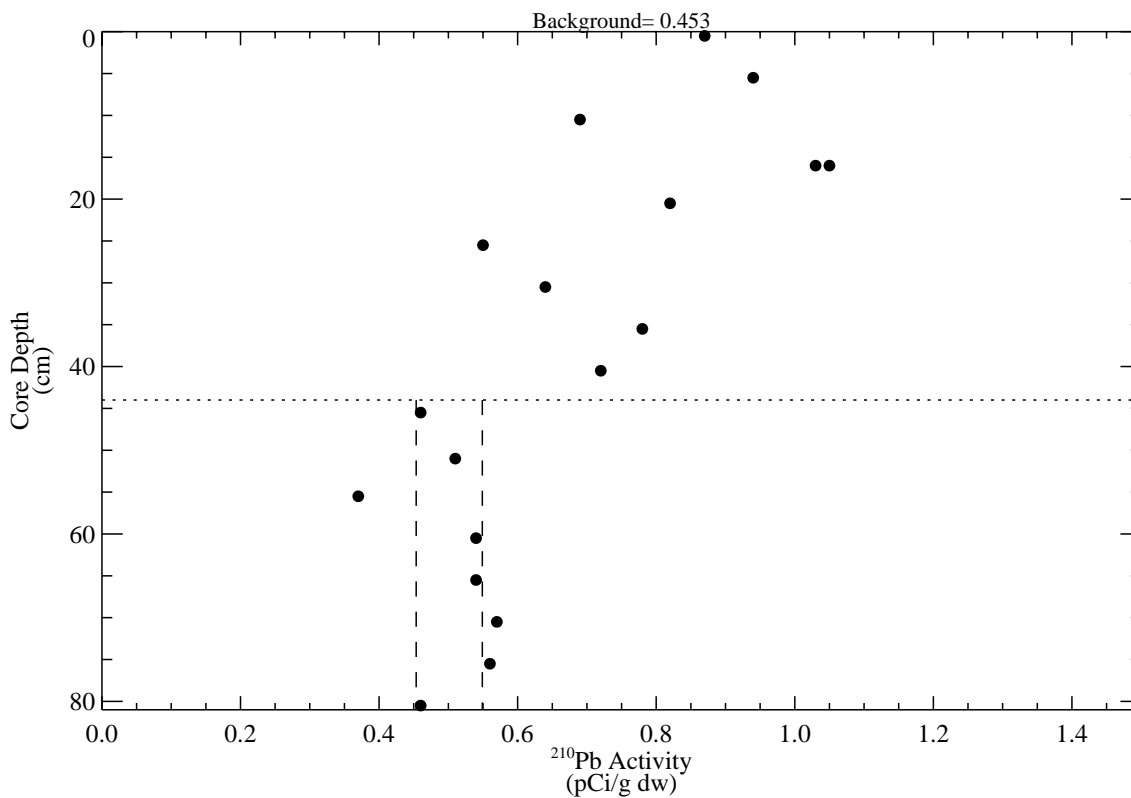


Figure E-23. ^{210}Pb levels as a function of sediment depth for core Sg-13.

Top panel: vertical distribution of ^{210}Pb activities. Data above dashed horizontal line used in sedimentation rate regression analysis. Vertical lines represent 95% confidence limits of supported ^{210}Pb activities used in regression analysis.

Bottom panel: natural logarithm of unsupported ^{210}Pb activities with depth. Dashed line represents slope of best fit regression.

Orange square symbols represent samples analyzed from archive.